Planar and Corner Reflectors Revisited

L. B. Cebik, W4RNL
1434 High Mesa Drive
Knoxville. TN 37938-4443
e-mail: cebik@cebik.com

Planar and corner reflectors have served communications since their invention in the late 1930s by John Kraus, W8JK. However, their life history almost disappears when television moved from direct broadcast to cable transmission and computer modeling allowed the development of Yagi designs to new and more assured levels of performance. As a result, handbook entries on planar and corner reflector arrays are decades old, and the most advanced array within the category dates to the early 1970s.

Even the most fundamental description of the array's fundamentals is severely out of date. In Kraus, *Antennas*, 2nd Ed. (McGraw-Hill, 1988), pp. 545-560, we find only the initial basis of the array's theoretical elaboration. Kraus develops the original calculations for planar and corner arrays using "the method of images," a technique that assumes perfectly conducting reflecting sheets of infinite extent. Although fully apt at the most general level of theorization, the technique begins to show its limitations the moment that we use a driver with a finite diameter, reflector planes with finite dimensions, or reflector surfaces that are not solid. Indeed, even by the turn into 1960, most planar and corner reflector ideas are emerging from field experiments. See, for example, the wide-band UHF television array in Johnson, *Antenna Engineering Handbook*, 3rd Ed. (McGraw-Hill, 1993), pp. 29-21 to 29-24.

As we move into the 21st century, perhaps it is time to revisit the planar and corner reflectors with an eye toward some systematic investigation. We have the proper tools for exploring more of the finite dimensions of these arrays, namely, reliable antenna modeling software. With this tool, we can examine in serial order a large number of variations in various array dimensions, and even probe differences in types of reflector construction.

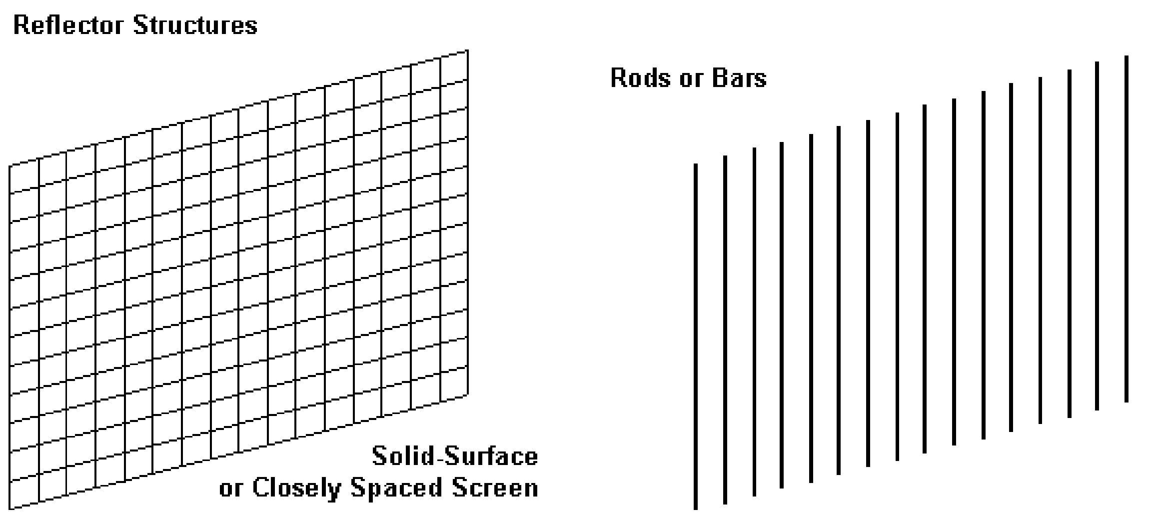

Fig. 1

Fig. 1 shows two types of typical reflector construction--applied for ease of viewing to planar reflectors. On the left is a representation of a modeled wire-grid structure that provides quite accurate results for reflectors composed of either closely spaced screening or solid surfaces. On the right is a typical bar or rod reflector. Traditional theory treats these two reflector types as equivalent so long as they meet certain standards and the outside dimensions are the same. As we shall discover, that assumption also is subject to significant limitations.

Because so many older assumptions grow less reliable as we begin to explore real materials and structures used in planar and corner reflector arrays, the following notes summarize work that will appear in a 9-part series in *antenneX* in 2005. The investigation involves carefully modeling a large number of arrays--literally hundreds of variations--in an effort to reach some general guidelines for specific designs. As with any investigation based on NEC-4 models, we shall be looking at two inter-related classes of issues: modeling issues and design issues. It is necessary to validate the techniques in the process of reaching some evaluation of the reliability of the results.

The study itself uses some working baselines in order to make its results as widely applicable as possible.

1. All but a few modeled arrays are designed for a 50-Ohm feedpoint impedance in view of the nearly universal amateur radio use of 50-Ohm feedlines. Other impedances are possible, and we shall note a few uses for them along the way.

2. All models in the study, like the rod reflector shown in **Fig. 1**, are vertically oriented, since the most likely applications for these arrays are communications services using vertically polarized antennas. However, since all models use a free-space environment, I shall provide both E-plane and H-plane values, wherever relevant, so that a horizontal application need only rotate the array by 90 degrees without losing the data presented.

3. All models use a design frequency of 299.7925 MHz so that 1 wavelength = 1 meter throughout. This procedure allows easy scaling by a factor of up to 10--up or down--without undue variation in the results owing to changes in element sizes for the driver assemblies.

4. All models use lossless (perfect) wire for ready comparisons from one model to the next. The elements are all fat enough so that the skin effect losses are minimal. For example, the difference between the maximum forward free-space gain for a typical lossless model and one composed of copper or aluminum is about 0.01-0.02 dB.

With these baselines established, we can go exploring.

Part 1: The Planar Reflector Array

We may view the planar reflector in two ways. The simpler way is to look at the reflector as a simple rectangular sheet. Alternatively, we can look at it as a special case of the corner reflector having an apex angle of 180 degrees. However, the simple sheet version may best suit our needs here, since it presents us (as well as our distant predecessors) with the opportunity to use a wide variety of driver assemblies, a feature not readily available to corner reflectors with 90-degree or tighter angles.

Essentially, we simply place a driven element or array in front of the reflector. **Fig. 2** shows the critical dimensions with which we shall be concerned. Not all of the dimensions are equally critical. For example, the exact length and height of the reflector itself may vary by 5% or so without significant change to performance, although changes of 1% to the driver or its spacing from the reflector may have noticeable effects on performance. However, despite the relative insensitivity of a reflector to dimensional change, there are limits. As well, there are differences between wire-grid and rod-based reflectors.

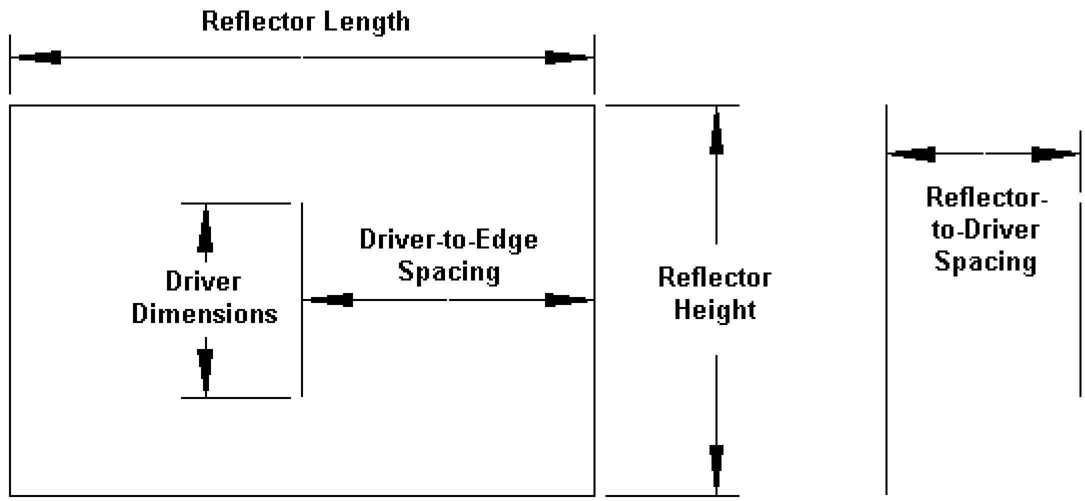

Planar Array Critical Dimensions

Fig. 2

Modeling Issues with Planar Reflectors

Modeling a planar reflector is not so simple a task as it seems. Each type of reflector presents challenges if the results are to be reliable.

1. The wire-grid reflector: The wire-grid modeling structures used for the investigation used standard grid construction. The length of each segment between junctions was 0.1 wavelength. The wire diameter used was the segment length divided by PI, or 0.0318-wavelength. To assure myself that these standard yielded reasonable simulations of closely spaced screens or solid surfaces, I used representative models and reduced the grid side lengths first by 2 and then by 4, reducing the grid wire diameter accordingly. In all test cases, the reported results varied only in the 4^{th} significant digit. Hence, at least internally, the tests provided a reasonable assurance that the basic wire-grid structures provide a good simulation of the intended physical objects.

2. The rod-based reflector: There are, in principle, no required special tests for a rod-based reflector. Its individual parts are each subject to standard NEC limits for round-wire structures, and all models stay well within those limits. However, there is an issue related to the assumption that rod-reflectors and solid-surface reflectors perform alike. The question then became finding a rod reflector that performs like a wire-grid model. My procedure was to develop a gain curve for a wire-grid reflector, accounting for its length and height with a simple dipole driver at a distance from the reflector that yielded a resonant 50-Ohm impedance at

peak gain. I then experimented with rod reflectors of the same outside dimensions, varying the diameter of the rods and the spacing between them. The goal was to find a combination of rod spacing and diameter that yielded a peak in gain with the same outer reflector dimensions, the same driver spacing from the reflector, and the same 50-Ohm impedance.

There is no single solution to the interaction of variables. For example, a combination of a 0.024-wavelength diameter and 0.0857-wavelength rod spacing produced good results, as did a combination of a 0.034-wavelength diameter and 0.12-wavelength spacing. However, the one I selected used rods having a 0.03-wavelength diameter. The rod spacing was a convenient 0.1-wavelength, which simplified the construction of the many modeled reflectors, both planar and corner. The required combination of rod diameter and spacing does represent a pair of interactive variables. As rod diameter increases, spacing also increases, and vice versa. At the same time, my selection of a combination uses spacing that is similar to traditional treatments, but a rod diameter between 50% and 100% fatter. However, traditional treatments are based on field experiments that establish only something that will work, not an equivalence between rod and solid reflector surfaces.

The solutions to both the wire-grid and rod reflector issues apply equally to both planar and corner reflectors, so this small discussion will not require repetition. Let's begin our exploration using only wire-grid reflector models to simulate closely spaced screens or solid surfaces.

Planar Reflectors and a Dipole Driver

Fig. 2 shows the most traditional planar reflector array: a reflector sheet and a simple dipole driver. I selected a relatively fat dipole: 8-mm diameter. The dipole required for a 50-Ohm feedpoint impedance is 0.436-wavelength long and spaced 0.175-wavelength from the reflector. One advantage of using a planar (or a corner) reflector is that the designer can adjust the spacing and the dipole length to achieve a desired resonant impedance (within limits) without disturbing performance figures. Hence, the arrays are relatively easy to field adjust to a desired passband.

One goal of the study was to discover whether there is an optimal size reflector that yields maximum performance from an array. I let the key factor be maximum gain, because the front-to-back ratio varies so slowly. In fact, at maximum gain, a simple dipole driver has a 180-degree front-to-back ratio of about 18 dB, with well-behaved rear lobes. The front-to-back ratio tends to increase with the reflector size to the largest size used in the study. That reflector was 2.0 wavelengths vertically by 2.0 wavelengths horizontally. The reflector sizes varied from that maximum down to 1.0 wavelength vertically by 1.0 wavelength horizontally. I used vertical and horizontal increments of 0.2 wavelength for each set of tests, for a total of 36 models per driver.

A simple dipole driver yields its maximum gain when the wire-grid planar reflector is 1.2 wavelengths vertically and 1.2 wavelengths horizontally. In **Fig. 3**, each graphed line represents a different horizontal size, while the X-axis records the progression of vertical sizes. The gain peak is fairly broad with respect to changes in the horizontal dimension, but somewhat more sensitive to changes in the vertical size. However, from a construction standpoint, neither dimension is hypercritical.

Of the drivers that we shall sample with a planar reflector, the dipole has the widest native (no-reflector) beamwidth in both the E-plane and the H-plane. Hence, its beamwidths tend to be higher and its forward gain lower than any other driver surveyed. However, a 9.3-dBi free-space gain utility array that is simple to construct and adjust might be very useful at 432 MHz and higher.

Fig. 3

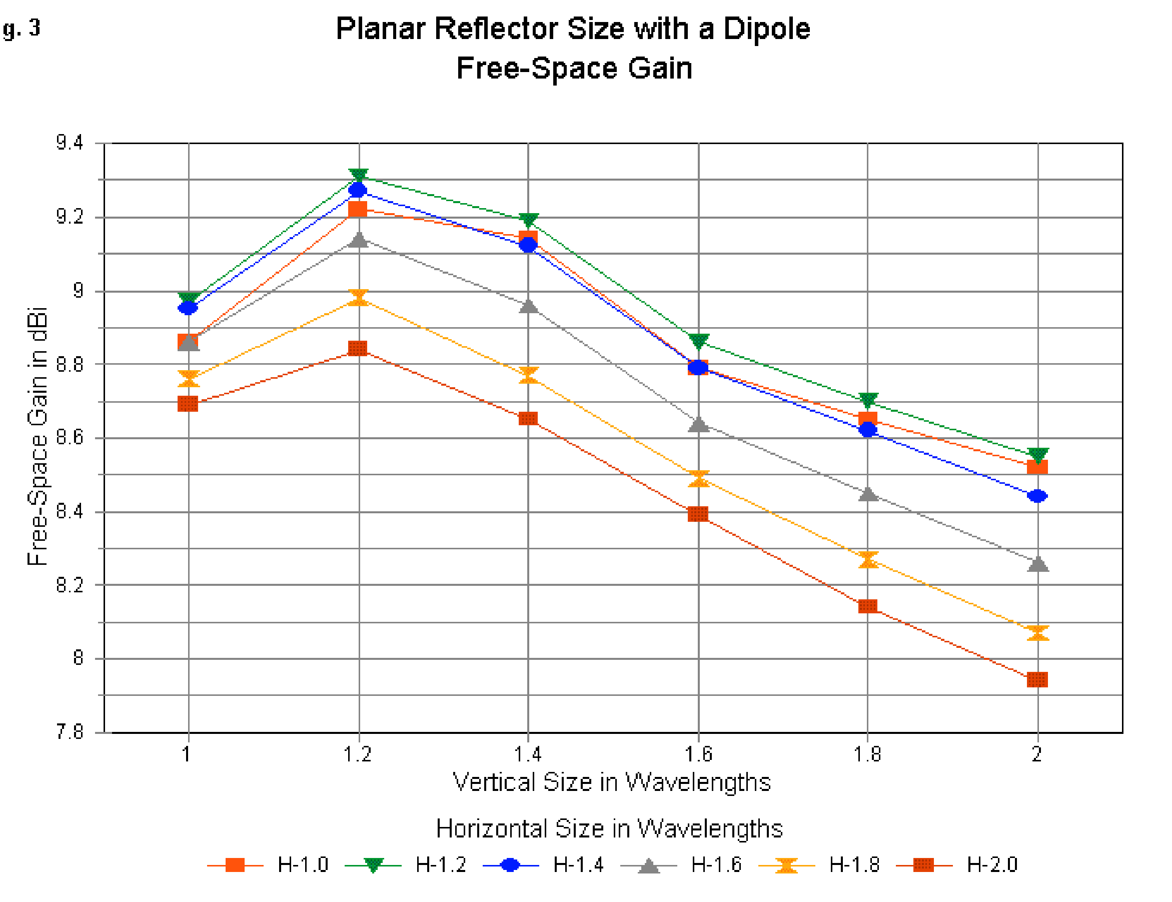

At maximum gain with a 1.2-wavelength by 1.2-wavelength reflector, I obtained the following performance reports. The front-to-back value is for 180 degrees. E-BW and H-BW are the -3-dB beamwidths for the E- and H-planes, respectively.

Free-Space Gain dBi	Front-to-Back Ratio dB	E-BW degrees	H-BW degrees	Impedance R +/- jX Ohms	50-Ohm SWR
9.31	18.33	54	80	49.72 - j0.15	1.01

The 2:1 50-Ohm SWR bandwidth for the simplest planar array is about 10% of the design frequency, enough to cover the 70-cm band. In fact, a second advantage of a planar array is that the feedpoint impedance and hence the SWR does not vary with the reflector size. **Fig. 4** presents the overlapping SWR curves for our 8-mm diameter dipole placed at the same position in front of 3 sizes of reflector.

However, the SWR bandwidth will change as we change the diameter of the driving dipole. **Fig. 5** supplies the SWR frequency sweep curves for 8-mm, 12-mm, and 16-mm dipoles, each adjusted in length and position for a 50-Ohm impedance at the design frequency. Changing dipole diameter does require a small change of position as well as length to establish the proper mutual coupling relative to the reflector--or, in other terms, the proper illumination of the reflector. However, the resulting increases in SWR bandwidth are small--about the same as for a dipole in isolation.

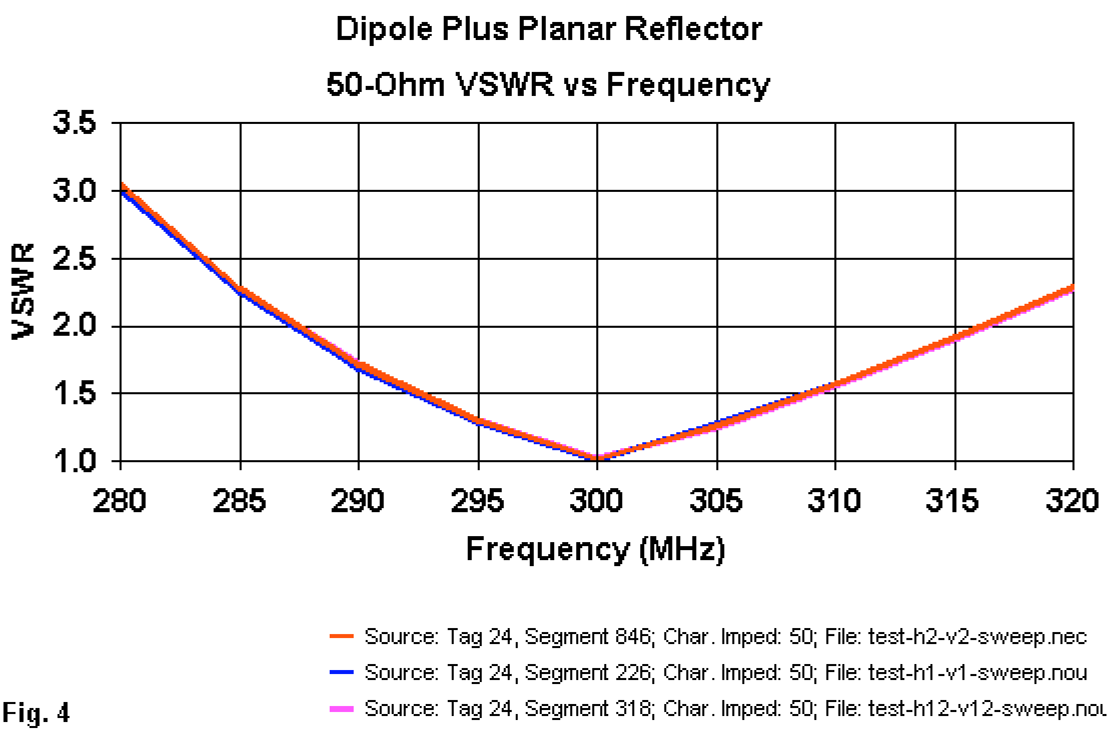

Fig. 4

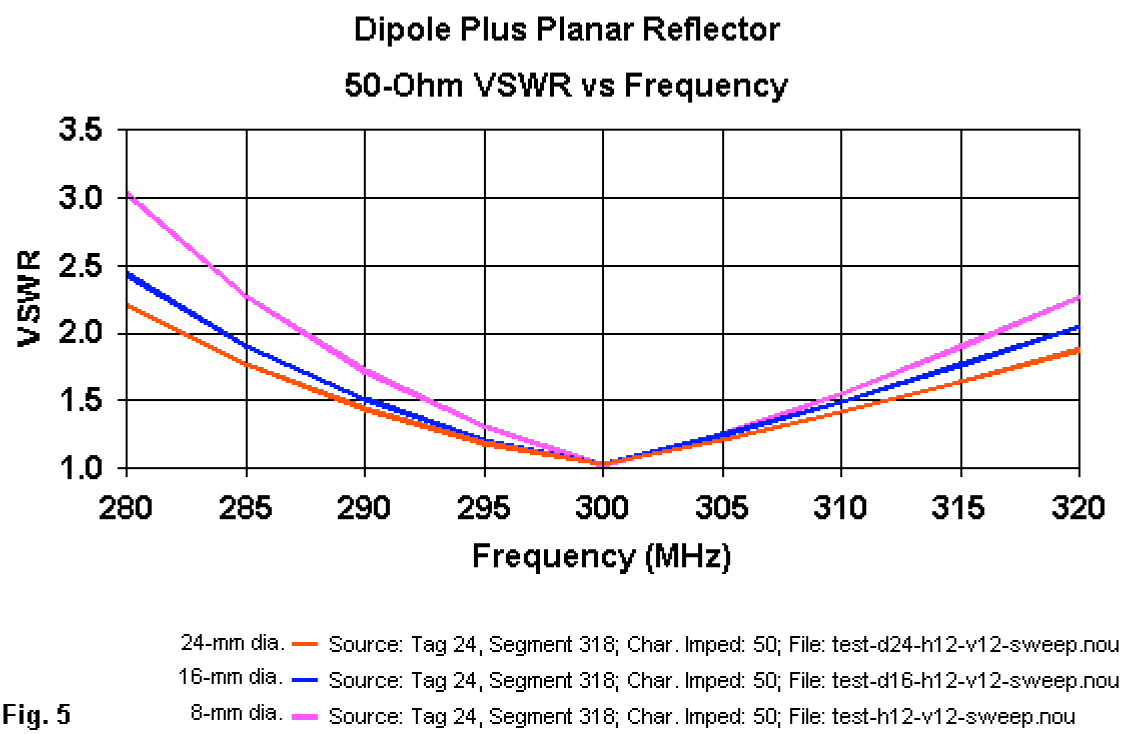

Fig. 5

Other Drivers, Other Numbers

On of the advantages of the planar reflector that other illuminated reflectors do not share is the ability to support any number of driver assemblies. Early on, Kraus himself imagined a practical "billboard" reflector with 8 phase-fed dipoles. More practical for contemporary VHF and UHF service are some smaller self-contained drivers using only a single feedpoint. In MF and HF service, many of these arrays belong to the class of wire antennas called self-contained vertical arrays or SCVs for short. When converted to our test frequency, using 4-mm diameter wire, and placed ahead of planar reflectors, the arrays take on dimensions shown in **Fig. 6** through **Fig. 9**.

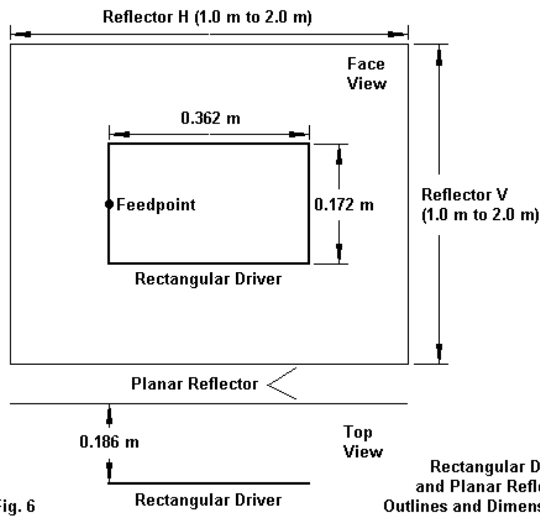

Fig. 6 Rectangular Driver and Planar Reflector Outlines and Dimensions

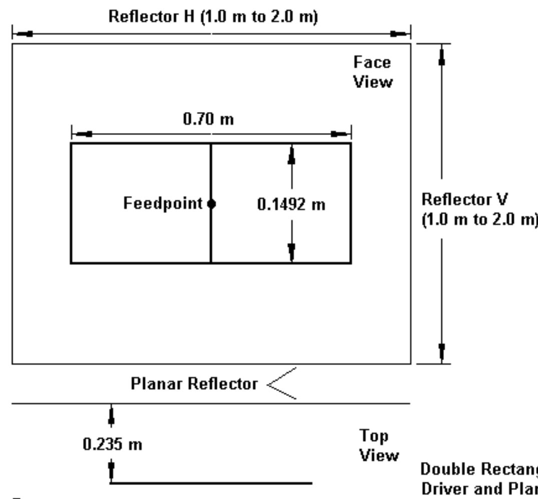

Fig. 7 Double Rectangle Driver and Planar Reflector Outlines

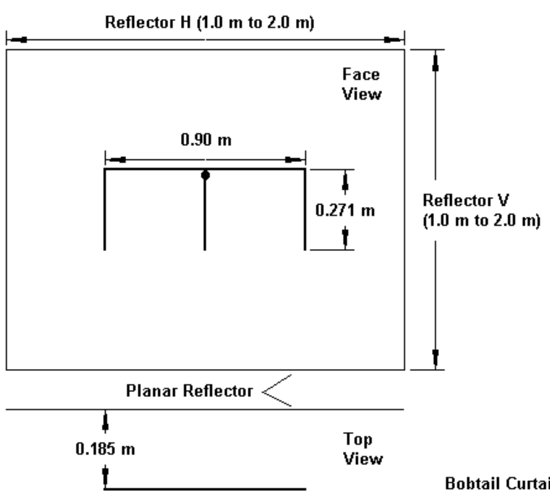

Fig. 8 Bobtail Curtain Driver and Planar Reflector Outlines

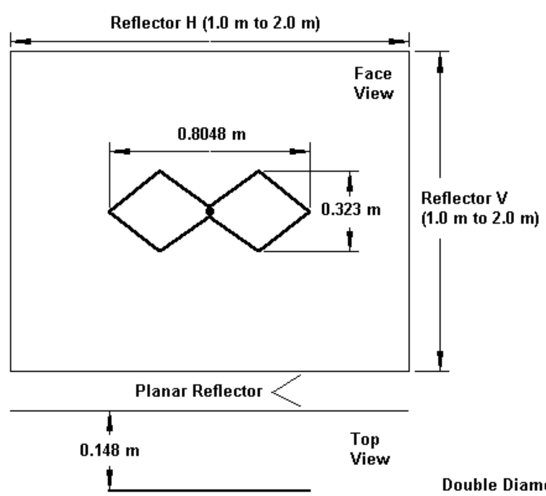

Fig. 9 Double Diamond Driver and Planar Reflector Outlines

Each driver requires a set of dimensions that, in isolation, maximizes bi-directional gain. Hence, most of these vertically polarized arrays are somewhat squat. That is to say, they are extended horizontally to approach a spacing of ½-wavelength between the high-current regions of the elements, thus shortening the vertical elements from a nominal ¼ wavelength. The spacing from the planar reflector for each driver derives from the inherent resonant feedpoint of the driver array in isolation. The lower the inherent impedance, the farther the array must be from the planar reflector to arrive at a resonant 50-Ohm impedance in planar array service.

In addition, each array requires, for maximum gain, a horizontal reflector dimension that is a function of the driver's horizontal dimension. In general, and within the increments used in the stepped modeling survey, the reflector must extend beyond the edge of the driver assembly by about 0.5 to 0.6 wavelength on each side, which corresponds roughly to the extensions for our initial dipole driver at its 1.2-wavelength optimal horizontal size. All of the driver assemblies reach maximum gain with a vertical reflector size of 1.2 wavelengths. The following table provides the optimal reflector dimensions.

Driver Type	Maximum Gain dBi	Vertical Reflector Dimension wl	Horizontal Reflector Dimension wl
Single Dipole	9.31	1.2	1.2
Single Rectangle	10.37	1.2	1.4
Double Rectangle	10.89	1.2	1.8
Bobtail Curtain	11.31	1.2	2.0
Double Diamond	11.13	1.2	1.6

The double diamond may appear to violate the reflector extension rule-of-thumb that we set up. However, the center of the high-current region is not the tip of the diamond, but about 2/3rd of the way between the physical vertical peak and the greatest horizontal extension. Using this position, the extension rule remains in force.

A more complete table of performance reports appears below. In all cases, the data is for the reflector yielding maximum gain. Like the dipole-driven array, the front-to-back ratio continues to increase with reflector size in each dimension up to the limits used in the survey. The dipole data is repeated for reference.

Free-Space Gain dBi	Front-to-Back Ratio dB	E-BW degrees	H-BW degrees	Impedance R +/- jX Ohms	50-Ohm SWR
Single Dipole					
9.31	18.33	54	80	49.72 - j0.15	1.01
Single Rectangle					
10.37	19.43	56	63	49.76 + j0.39	1.01
Double Rectangle					
10.90	19.31	58	54	49.58 - j0.37	1.01
Bobtail Curtain					
11.31	21.45	58	48	49.95 + j3.23	1.07
Double Diamond					
11.13	21.22	56	52	49.63 - j0.65	1.02

The apparent winner in the gain "race" is the bobtail curtain driver. However, this driver is not balanced vertically, since the active vertical elements are ¼-wavelength monopoles. The result is a bit of wavering in the E-planar axis of maximum radiation--as much as 6-7 degrees above or below true horizon, depending upon the reflector size. The double diamond and the double rectangle have completely normal patterns, with the double rectangle being perhaps the easiest complex driver to implement physically.

There is little to choose with respect to both E-plane and H-plane beamwidth among the complex driver assemblies. Similar remarks apply to the 2:1 50-Ohm SWR bandwidth for the arrays, with the exception of the single rectangle. Its bandwidth is only about 4.7%, short of covering the entire 6.8% bandwidth of the 70-cm amateur band. In contrast, the other 3 driver assemblies show bandwidths of 7% to 8.7%, using 4-mm wire for the driver.

More Bandwidth

I have saved one complex driver assembly for last, because it is capable of approaching the gain level of the best of the survey, but offers a bandwidth about 3 times greater. Let's place two 8-mm diameter dipoles ½ wavelength apart and feed them in phase. **Fig. 10** shows the general outline of the array.

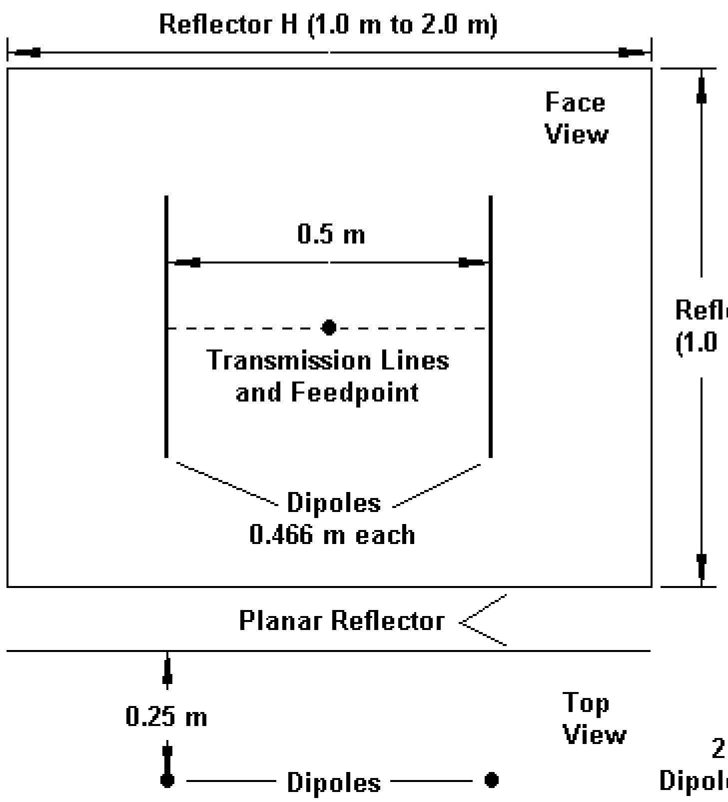

Fig. 10

2 In-Phase-Fed Dipoles and Planar Reflector Outlines

The spacing of the dipoles from the reflector is set to yield individual dipole impedances of 100 Ohms resonant. Each dipole connects to a center feedpoint junction by a 100-Ohm parallel transmission line, which one can fabricate from square stock or etch on a circuit board. The parallel combination at the single feed port yields 50 Ohms over a considerable band spread.

Fig. 11 provides a graph of the free-space forward gain of the array, and shows that a reflector that is 1.2 wavelengths vertical by 1.6 wavelengths horizontally is optimal for forward gain. Within the increment steps used in the survey, the horizontal dimension preserves the reflector horizontal extension rule noted earlier. However, the horizontal dimension proves very non-critical, since the lines for 1.4, 1.6, and 1.8 wavelengths very nearly overlay each other. As is the case with all of the complex drivers, gain peaks noticeably with a vertical height of 1.2 wavelength.

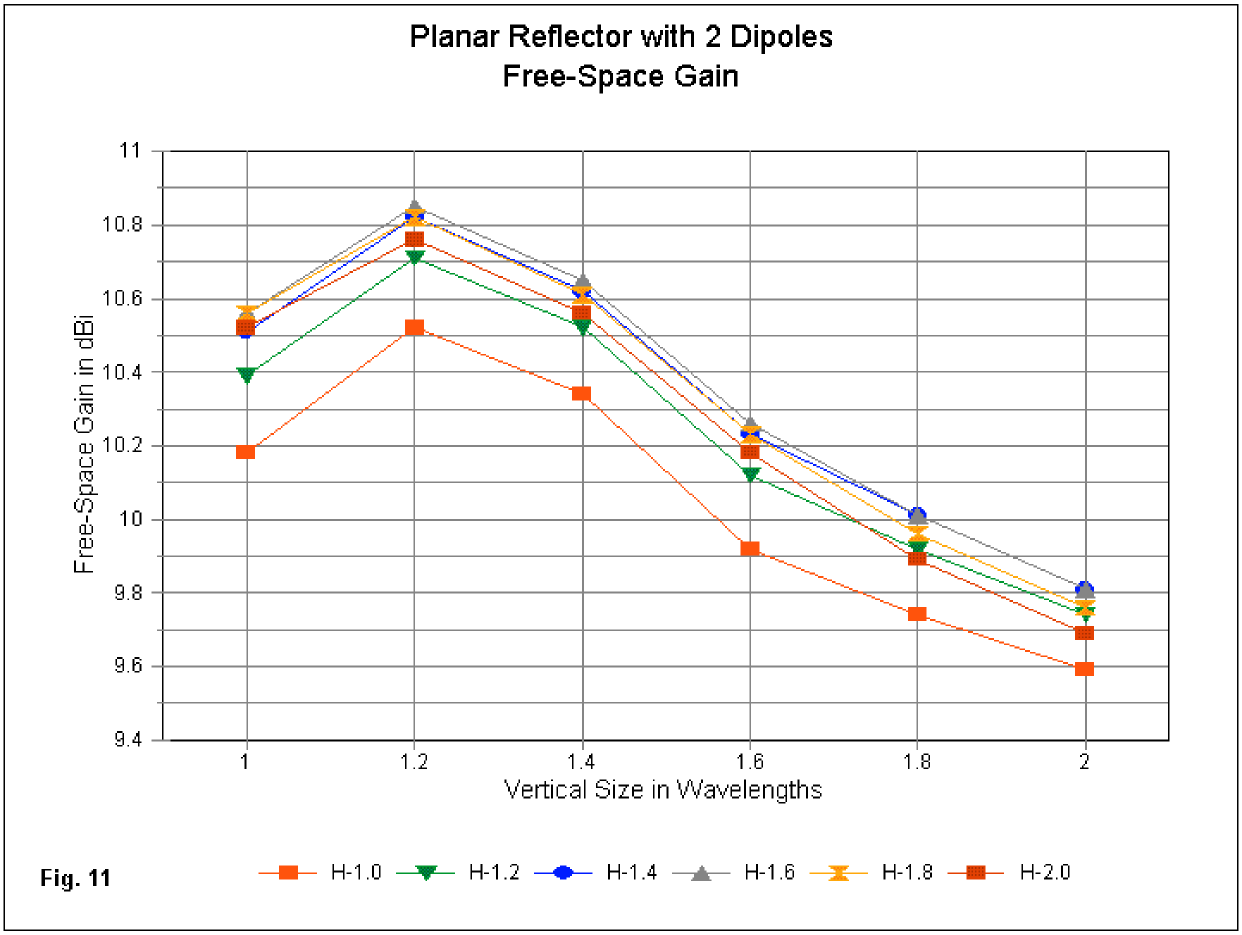

Fig. 11

The detailed performance values for a planar reflector array using 2 dipoles fed in phase appear in the next lines. The impedance value shown is for each dipole prior to the addition of the phase lines.

Free-Space Gain dBi	Front-to-Back Ratio dB	E-BW degrees	H-BW degrees	Impedance R +/- jX Ohms	100-Ohm SWR
10.82	19.56	58	54	97.77 - j2.25	1.03

As shown in the VSWR graph in **Fig. 12**, when we combine the phase lines, the 2:1 50-Ohm SWR limits extend from about 270 MHz to nearly 350 MHz. The span is just shy of 80 MHz, or about 26% when related to the design frequency. Like all such graphs, the SWR increases more rapidly below the design frequency than above it, so the true mid-band point is about 310 MHz.

The SWR bandwidth is accompanied by relatively flat performance figures. For all of the complex drivers, performance holds up well beyond the SWR limits. For the in-phase-fed dipoles, we end up with an array that would not merely cover the 70-cm band, but when scaled in another direction, easily cover the entire FM broadcast band. The free-space gain of nearly 11 dBi is very good for an antenna in the utility class, with applications extending from the upper VHF range through the upper UHF range. The similarity of beamwidths in both the E-and the H-planes means that rotating the antenna 90-degrees for a horizontal application will yield results equal to those in vertical applications.

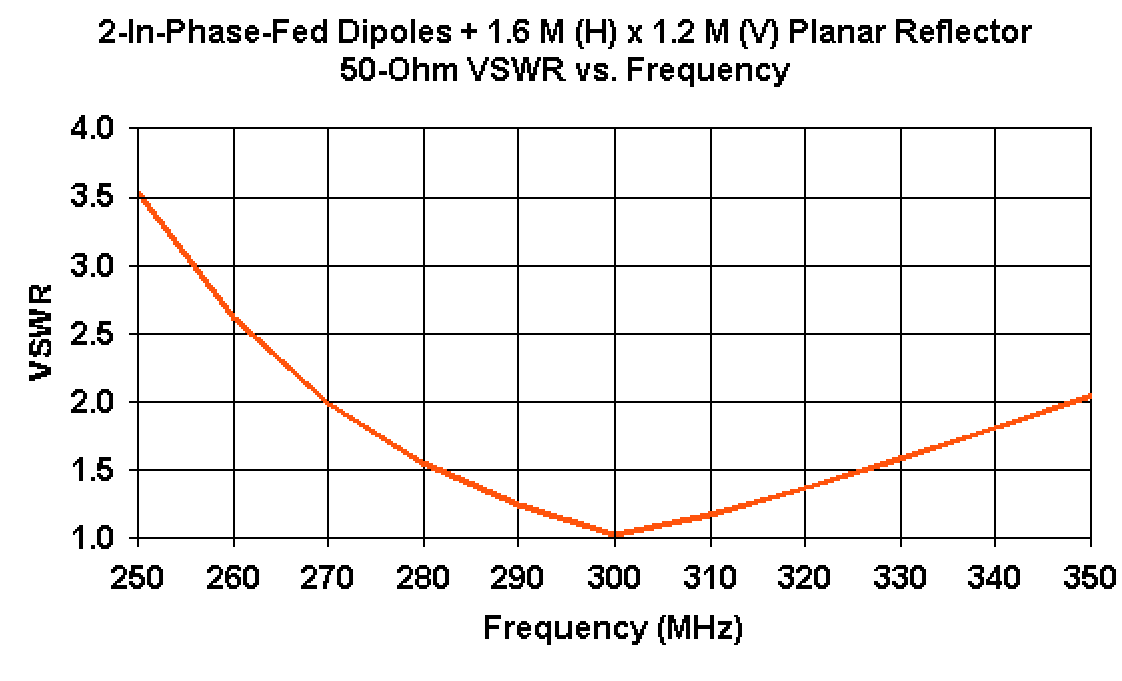

Fig. 12

From Wire-Grid to Rod Reflectors

All of the reports that we have examined apply to models using wire-grid reflector structures to simulate reflectors that use solid surfaces or closely spaced screens. We may replace the wire-grid reflectors with rod-based reflectors. The resulting arrays will perform very much like their wire-grid cousins when we optimize the vertical dimension at 1.2 wavelengths. In all cases, the required horizontal dimension for maximum gain is identical for both types of reflector structures. The following table compares the performance of all of the arrays using both types of reflectors, with the wire-grid version listed first.

Free-Space Gain dBi	Front-to-Back Ratio dB	E-BW degrees	H-BW degrees	Impedance R +/- jX Ohms	50-Ohm SWR
Single Dipole					
9.31	18.33	54	80	49.72 - j0.15	1.01
9.27	18.24	54	80	50.01 + j0.09	1.00
Single Rectangle					
10.37	19.43	56	63	49.76 + j0.39	1.01
10.23	19.11	56	59	49.98 + j0.15	1.00
Double Rectangle					
10.90	19.31	58	54	49.58 - j0.37	1.01
10.83	19.18	58	52	50.25 - j0.29	1.01

Bobtail Curtain					
11.31	21.45	58	48	49.95 + j3.23	1.07
11.21	21.23	57	44	50.11 + j0.11	1.00
Double Diamond					
11.13	21.22	56	52	49.63 - j0.65	1.02
11.02	20.88	56	50	49.93 + j1.41	1.03
2 Dipoles Fed In Phase					
10.82	19.56	58	54	97.77 - j2.25	1.03
10.79	19.23	58	54	99.99 - j0.17	1.00

(Note: Phased Dipole SWR Values are relative to 100 Ohms.)

In all cases, the rod-reflector shows a very slight gain deficit relative to the wire-grid reflector version of the model. In no case is the deficit within normal operational detectability. As well, some rod reflector arrays shows a slightly narrower H-Plane beamwidth. Although not severe, the beamwidth narrowing is a prelude to an anomaly that occurs with some driver assemblies if we increase the vertical dimension to 1.4 wavelengths. **Fig. 13** compares the patterns in both planes for a simple dipole driver using each kind of reflector with a lower vertical height. Except for a very small difference in the H-plane just over 90 degrees from the forward heading, the two patterns are identical.

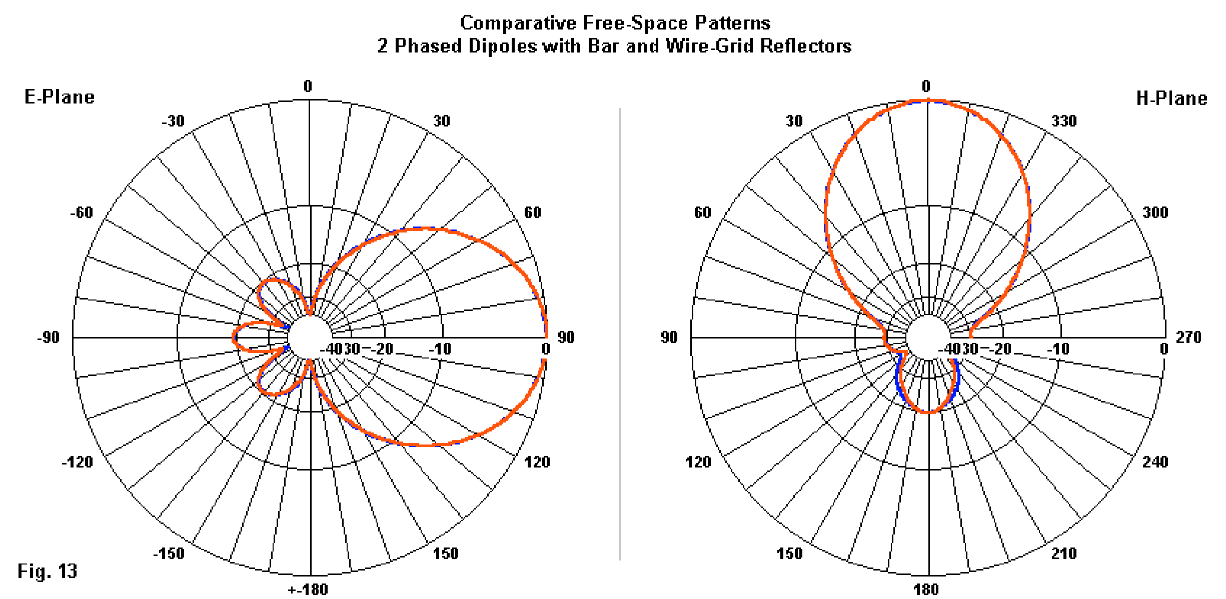

Fig. 13

The patterns will also serve as stand-ins for the patterns for all of the arrays, regardless of the driver complexity. Using reflector optimized for each driver, we obtain almost identical patterns, adjusted for the slight differences in gain and front-to-back ratio. However, if we set the vertical height of the reflector at 1.4 wavelengths and select the single rectangle as our driver, we find a different situation. **Fig. 14** compares wire-grid and rod reflector patterns for this situation, again in both the E- and H-planes. The well-behaved pattern belongs to the wire-grid reflector. The rod reflector produces a sudden drop in forward gain and a widening of the beamwidth in both planes. In the E-plane, the rear lobe structure enlarges, while in the H-plane, the pattern develops very large sidelobes to go with an enlarged rearward structure. Similar pattern distortions occur with a rod-reflector vertical dimension of 1.4 wavelengths using the bobtail curtain and the double diamond driver assemblies. However, the effect is absent from the single dipole, the in-phase-fed dipoles, and the double rectangle.

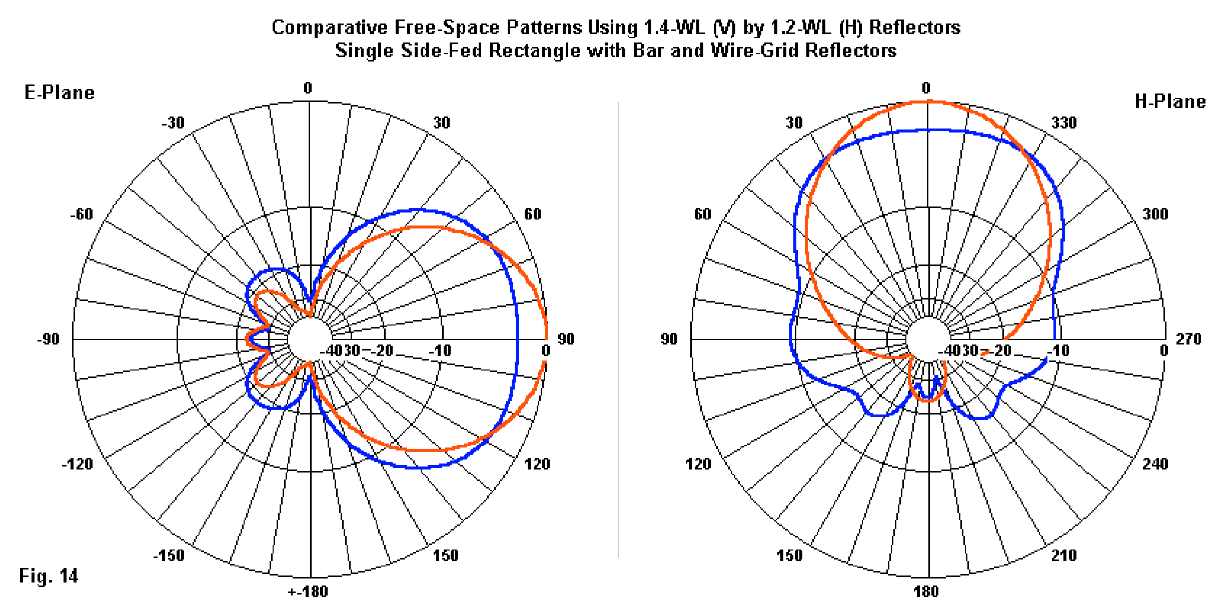

The phenomenon results from a combination of two factors: inherent driver bi-directional gain and the degree of coupling to the reflector rods. Each reflector rod at 1.4 wavelengths is nearly resonant at an odd multiple of a half wavelength. Hence, it is sensitive to parasitic effects as well as to the illumination effects that we find in a wire-grid reflector. However, to trigger the effect, we must also have sufficient gain directed toward the reflector at a spacing that enhances parasitic coupling. For our sample drivers, the dipole has a spacing below 0.2 wavelength, but does not have sufficient gain to do other than illuminate the reflector. The dual-dipoles and the double rectangle use spacing greater than 0.2 wavelength and hence do not over-couple to the reflector. However, the single rectangle, bobtail curtain, and double diamond all require spacing from the reflector that is well under 0.2 wavelength, but with sufficient gain to yield parasitic coupling.

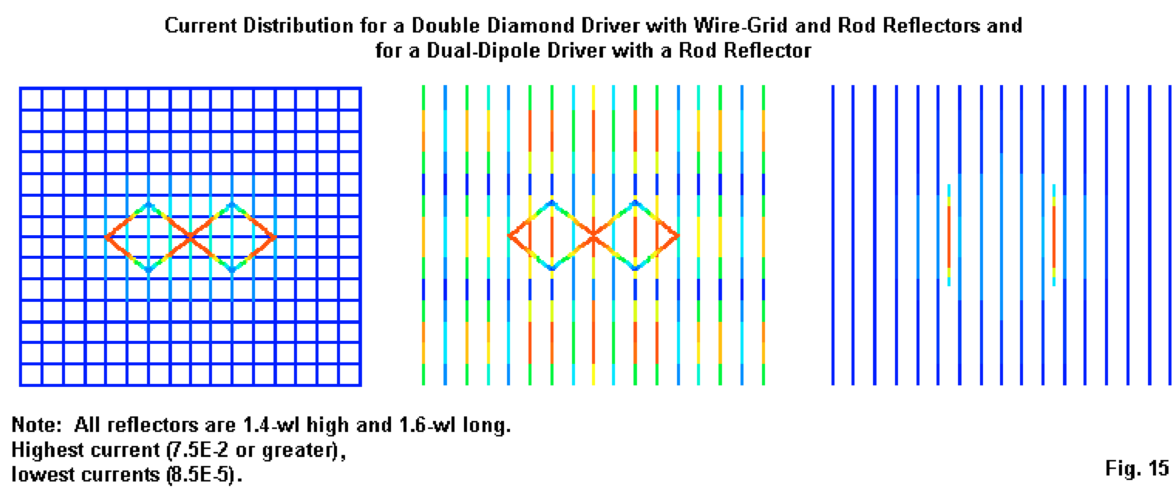

Fig. 15 contrasts three cases by showing color representations of the current magnitude distribution on the reflectors that are 1.4 wavelength high. In gray-scale rendering, the contrasts are not as vivid, but are still readable. The double diamond, with a wire-grid reflector,

shows even illumination of the reflector, as indicated by the same line-darkness, except immediately behind the driver. A similar situation applies to the rod reflector with the dual-dipole driver: the rods all have the same line darkness except immediately behind each dipole. The center graphic, which shows a double diamond with a rod reflector, tells a far different tale. The changes in line darkness show peaks and nulls in current along the reflector rods, with the darkest portions alternating between the highest currents (red in the original) and the lowest currents (deep blue in the original). Gray areas show intermediate current levels.

The end result is a caution and a foreshadowing of things to come. If using a rod-based reflector structure, maintain a vertical height of not greater than 1.2 wavelengths or so at the highest frequency used by the array. The recommended height limit yields the highest array gain for any driver assembly (excepting possible collinear arrangements). This statement about maximum gain will not apply to corner reflectors, so we may anticipate a more complex situation when we turn to them.

Summarizing Planar Reflectors

Before turning the corner, we may summarize our findings about planar reflectors.

1. The feedpoint properties of any driver so far, once established, remain the same regardless of the reflector size. Across the span of 36 reflectors used in the exercise, the maximum change in 50-Ohm SWR was from 1.01:1 to 1.09:1, although a range of 1.01:1 to 1.04:1 is more typical.

2. The ideal maximum gain height of the reflector is about 1.2 wavelength, regardless of the driver vertical or horizontal dimension. The actual "ideal" vertical dimension may be closer to 1.3 wavelength, but should not reach 1.4 wavelengths with rod reflectors.

3. The ideal maximum gain reflector is one that extends horizontally beyond the driver system by about 0.5 to 0.6 wavelength.

4. The phase-fed dual-dipole driver provides the widest SWR passband of any driver assembly, and at a good gain level. However, the other driver systems all offer somewhat simpler construction and fewer field adjustment challenges.

5. The bobtail curtain and the double diamond driver systems provide the maximum gain from a planar reflector array. However, almost all of the driver systems provide gain equal to what we might derive from various long-boom 5-6 element Yagis.

6. In none of the arrays does the maximum front-to-back ratio coincide with the maximum gain in terms of reflector size. If we use a front-to-rear ratio, averaging the rearward gain across the 180 degrees of rearward directions, it appears that the larger the reflector, the lower the average rearward gain and the higher the front-to-rear ratio.

7. E-plane beamwidth is generally controllable by the selection of the horizontal reflector dimension. H-plane beamwidth, once beyond the single dipole driver, is relatively constant and lacks the secondary forward sidelobes that are typical of Yagis in the same gain category.

Planar reflector arrays show considerable potential for easily constructed utility arrays for both amateur and other services. Before the universalization of cable television, they once served atop many households for UHF stations. Perhaps they now deserve a place on amateur masts and towers.

Part 2: Corner Reflectors

The corner reflector is at once simpler and more complex than the planar reflector. Unlike the planar reflector, the tight confines between the angled corner reflector surfaces do not permit much variation in the type of driver that we may use. We shall limit ourselves to variations on the dipole. At the same time, the corner reflector itself has a much larger number of variables than the planar reflector. **Fig. 16** displays some of them, grouped according to those that are solely a function of the reflector structure and those that involve the relationship of the reflector and the driver.

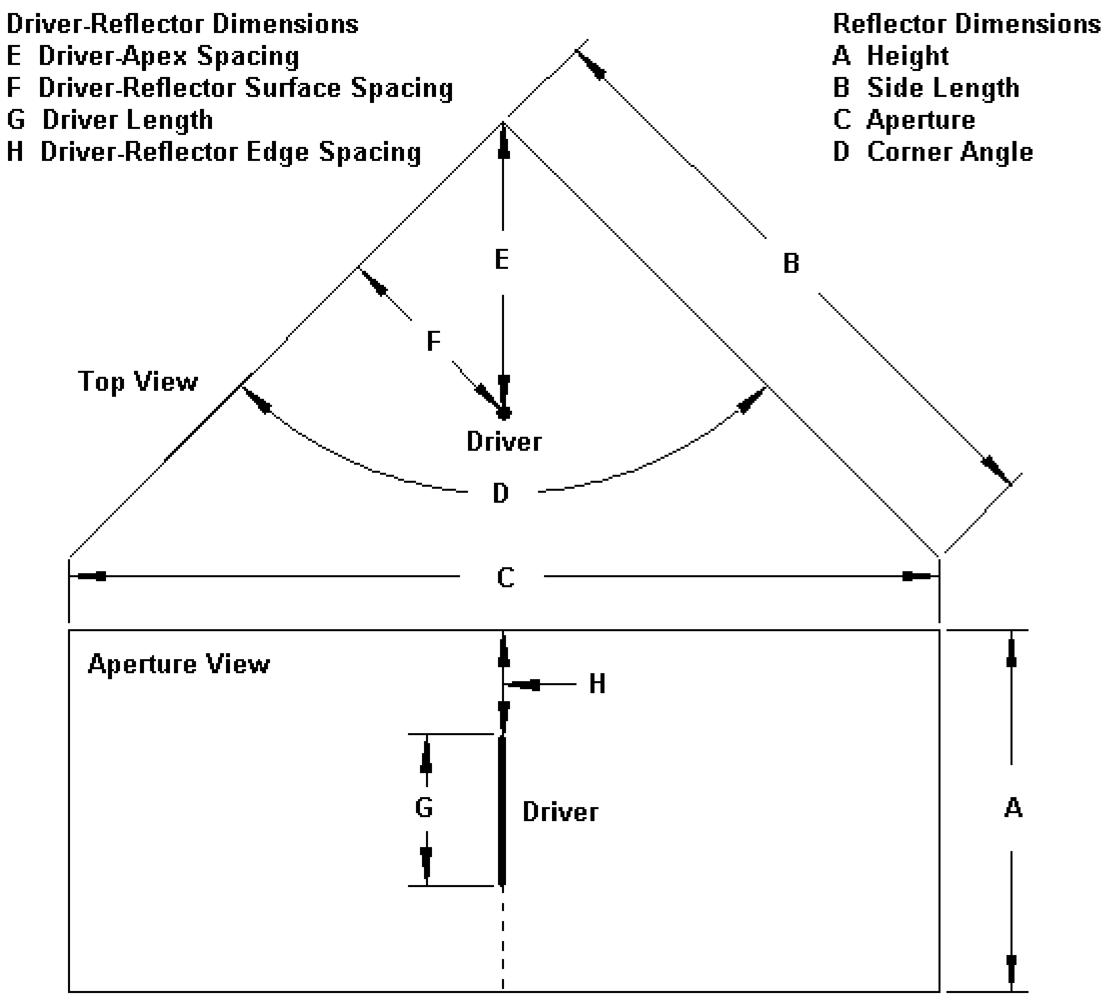

Corner Reflector Critical Dimensions

Fig. 16

The pure reflector properties include dimensions A through D: the vertical or E-plane height, the side length, and the corner angle. Together, the corner angle and the side length determine the aperture. Most past corner reflectors have used a 90-degree angle, and we shall adhere to this tradition for much--but by no means all--of our investigation. Initially, we shall be very much concerned to see the relationship among the E-plane height, the side length, and array gain. The dimensions noted here are a standard part of traditional corner reflector treatments. Once we introduce a driver--normally, a simple dipole--dimensions E through H capture our attention. The distance from the dipole to the corner apex has been a standard measure. However, in tests with different diameter dipoles, this distance changes, but results in a dipole-surface-to-reflector-surface distance that almost does not change at all. The driver length (whether a simple driver or something more complex) turns out to have a bearing on the required height of the reflector, giving the driver-end-to-reflector-edge dimension some significance. As with planar reflectors, we shall also be interested in differences that may appear when switching from a wire-grid reflector model to a rod-based reflector model. Except for the distance between the driver and the corner apex, traditional literature tends not to treat the members of this latter group of dimensions.

Corner Reflector Size

Fig. 17

Extremes of Corner-Reflector + Dipole Maximum Gain Free-Space Patterns
Reflector Aperture = 1.414 x Single Horizontal Dimension

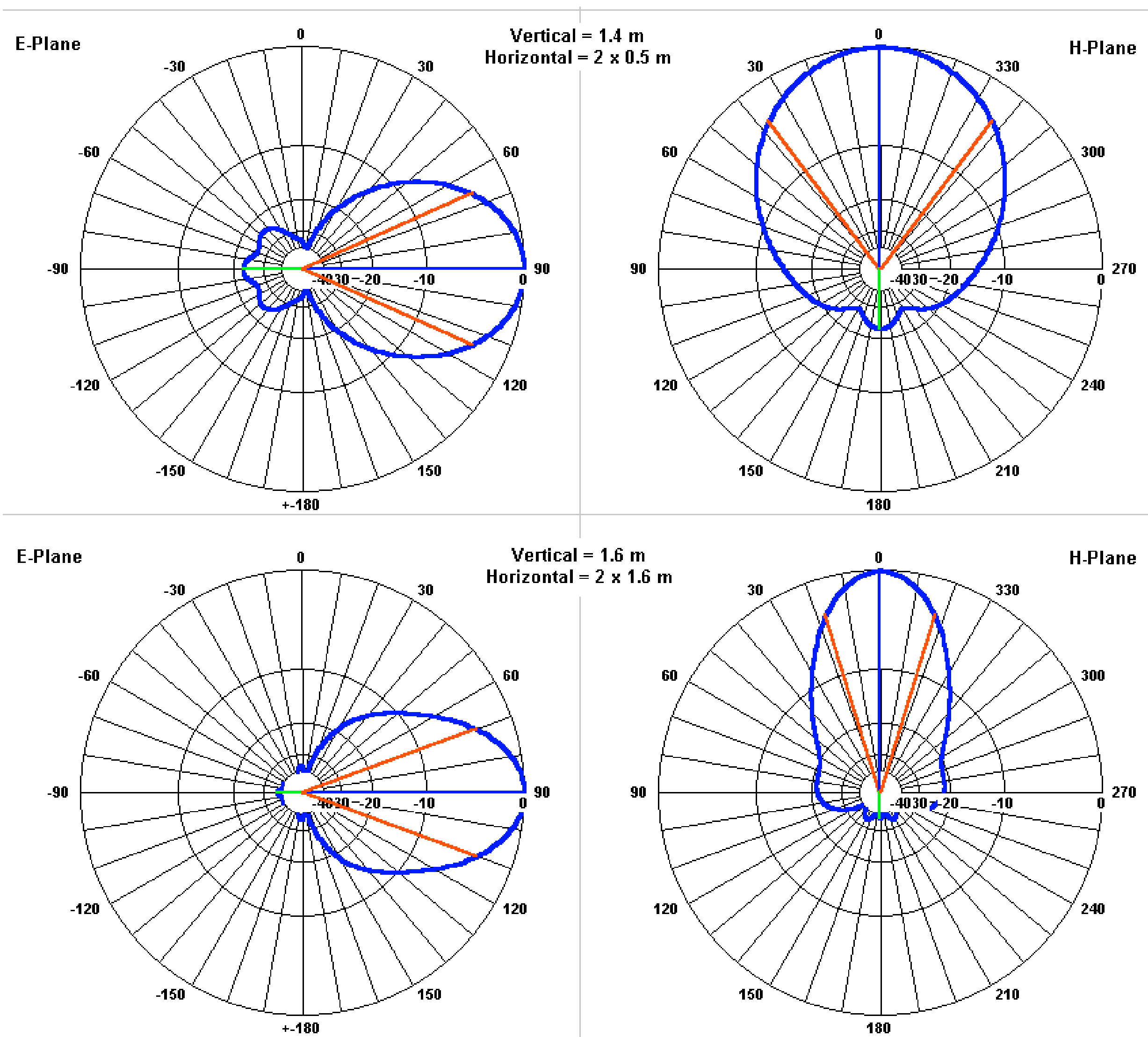

Regardless of the vertical height or the side length of a corner reflector, the array tends to yield an exceptionally clean set of E-plane and H-plane patterns, as shown in **Fig. 17**. As we move from very small reflectors toward much large ones, we gradually narrow the E-plane pattern. However, the H-plane pattern narrows more rapidly. For all vertical heights, increasing the side length from a very small 0.5 wavelength up to about 1.6 wavelengths decreases the H-plane beamwidth from 75 degrees down to about 35 degrees, with further but slower reductions for even longer side lengths.

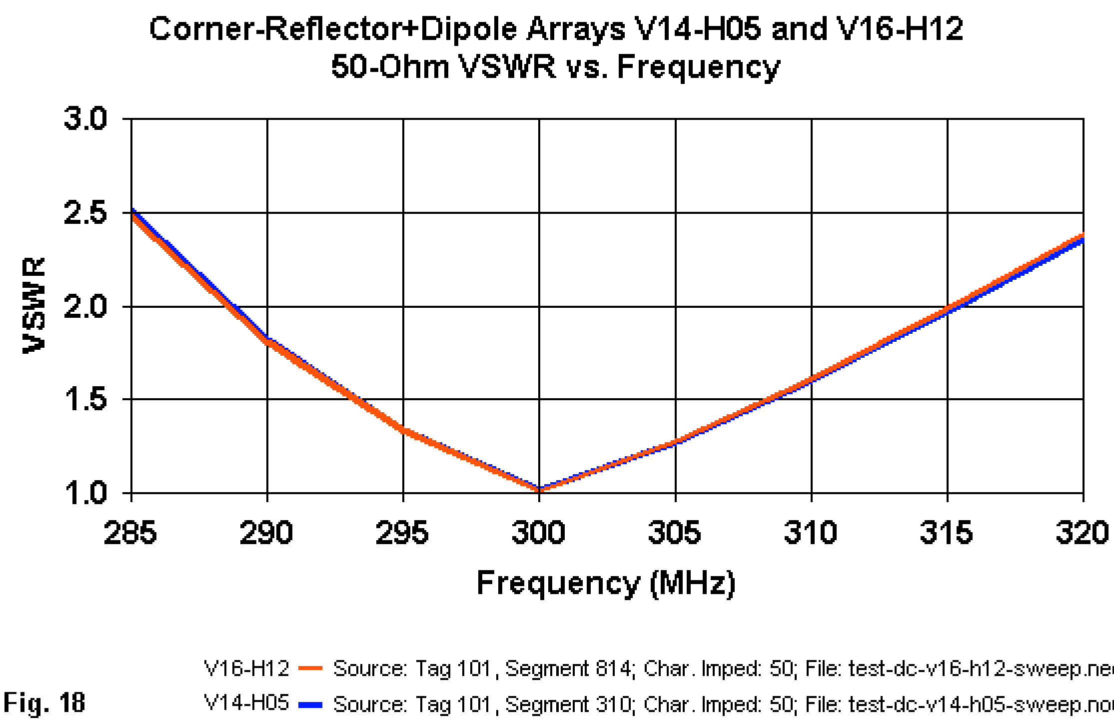

Fig. 18

Also regardless of reflector size, once we position a dipole driver, its impedance and SWR bandwidth do not change significantly. **Fig. 18** overlays the 50-Ohm SWR curves for 2 very different reflector sizes, and the result is at most a fat line encompassing the tiny differences between them. Hence, all of our initial corner reflectors can use a simple dipole that is 8 mm in diameter and about 0.324 wavelength from the apex. The required length is about 0.424 wavelength at our test frequency of 299.7925 MHz, where 1 wavelength = 1 meter. The placement establishes the 50-Ohm resonant feedpoint impedance that has been the standard throughout this study.

In light of past amateur and commercial practice, which employed somewhat skimpy VHF reflectors, I began the survey of wire-grid reflectors using a range of vertical heights between 1.0 wavelength and 2.0 wavelengths in 0.2-wavelength increments. Side lengths ranged from 0.5 wavelength to 1.6 wavelengths at 0.1-wavelength increments. Although useful in tracking some basic properties, the side lengths selected for detailed analysis proved insufficient to capture the reflector size needed for maximum gain. See **Fig. 19**. So I extended the side lengths, using larger increments, and **Fig. 20** resulted from the added work. (Some of the larger wire-grid reflectors require a few thousand segments for NEC-4 modeling, using the standard size wire grid established for planar reflectors.)

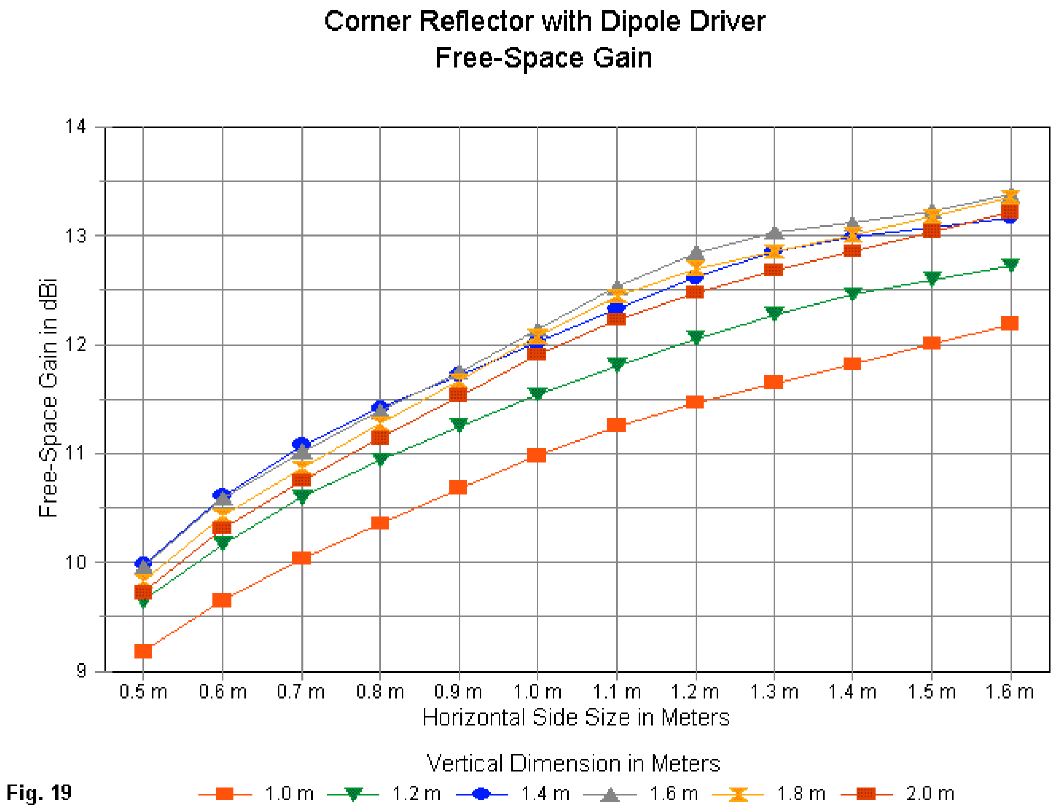
Corner Reflector with Dipole Driver
Free-Space Gain
14
13
12
11
10
9
Free-Space Gain in dBi
0.5 m
0.6 m
0.7 m
0.8 m
0.9 m
1.0 m
1.1 m
1.2 m
1.3 m
1.4 m
1.5 m
1.6 m
Horizontal Side Size in Meters
Vertical Dimension in Meters
1.0 m
1.2 m
1.4 m
1.6 m
1.8 m
2.0 m

Fig. 19

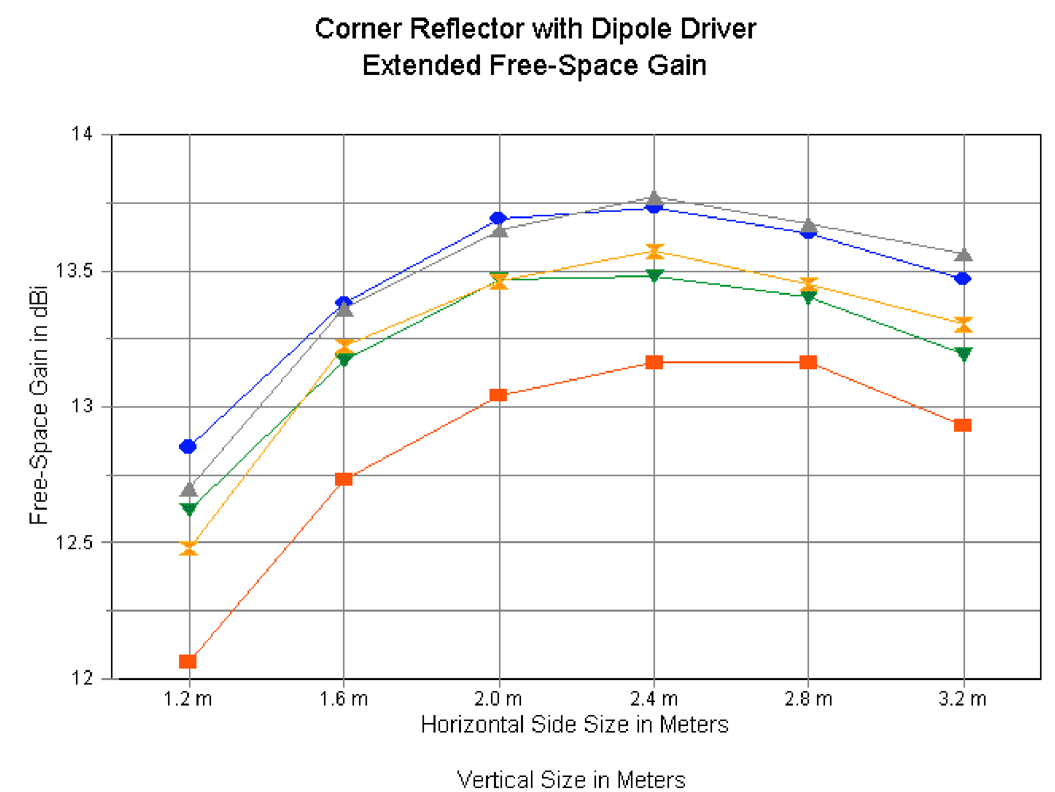
Corner Reflector with Dipole Driver
Extended Free-Space Gain
14
13.5
13
12.5
12
Free-Space Gain in dBi
1.2 m
1.6 m
2.0 m
2.4 m
2.8 m
3.2 m
Horizontal Side Size in Meters
Vertical Size in Meters
1.2 m
1.4 m
1.6 m
1.8 m
2.0 m

Fig. 20

The initial phase of the survey showed that a corner reflector requires considerably more height for maximum gain than a planar reflector. As well, since the curves continued to climb at the right edge of **Fig. 19**, maximum gain would require a significantly longer side length than virtually all past amateur builders had suspected. In the end, **Fig. 20** revealed that a vertical height of about 1.8 wavelengths combined with a side length of about 2.4 wavelengths yields maximum gain from a 90-degree corner reflector. At the same side length, a height of 1.6 wavelengths is almost as good. Hence, we might infer that 1.7-wavelengths might show a gain slightly and undetectably higher than the 13.76-dBi free-space maximum on the plot. Although I shall not display the graph here, the front-to-back ratio rises in accord with the gain. Whether additional gain will re-appear with very long (4- to 12-wavelength) reflectors, I did not explore, given the model sizes required.

Drivers and Bandwidth

Changing the diameter of the dipole driver affects the SWR bandwidth only a little. **Fig. 21** shows the 50-Ohm SWR curves for dipole diameters of 8, 12, and 16 mm. As we increase the dipole diameter, the length grows shorter, shrinking from 0.424 wavelength for the thinnest of the group to 0.407 wavelength for the fattest. As well, the spacing from the apex increases by 2 mm for each diameter increase, which maintains an almost constant closest approach between the driver and reflector surfaces. However, the 2:1 SWR bandwidths only increase from 9% to 10% to 11.7% across that 2:1 diameter range.

Fig. 21

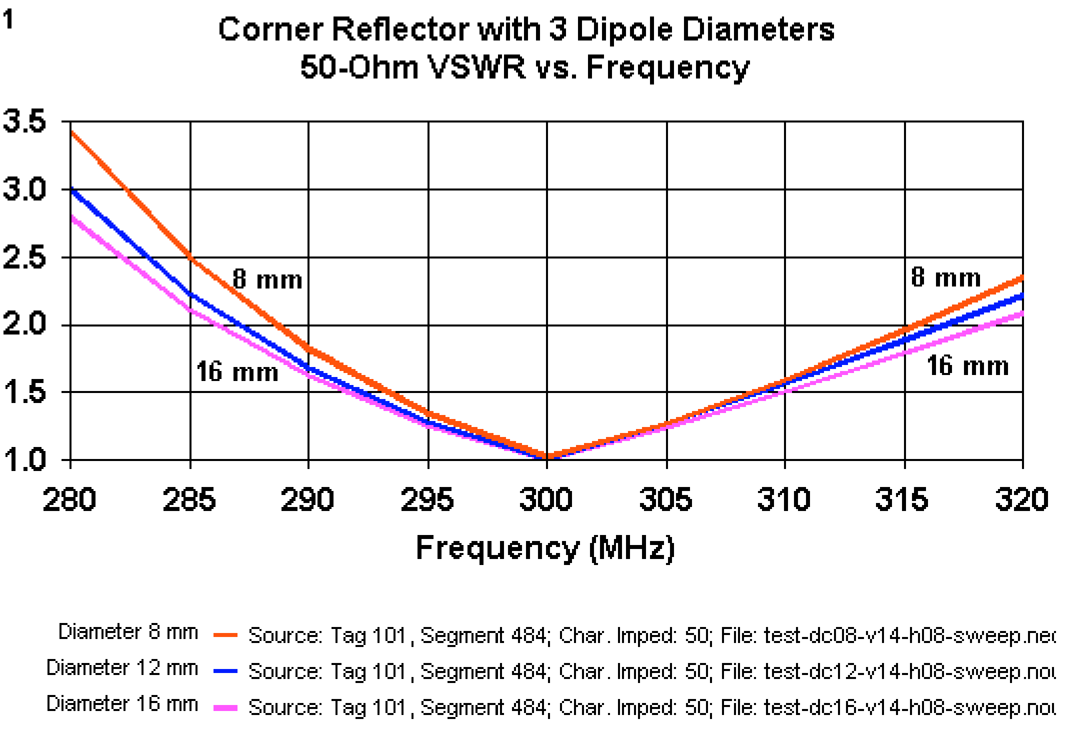

A more promising tactic is to increase the spacing of the driver from the corner reflector's apex. In the process, we also increase the resonant feedpoint impedance. **Fig. 22** shows the positions and lengths of three 8-mm drivers used to test the relationship between dipole position and impedance on the one hand and the SWR bandwidth on the other.

Fig. 22

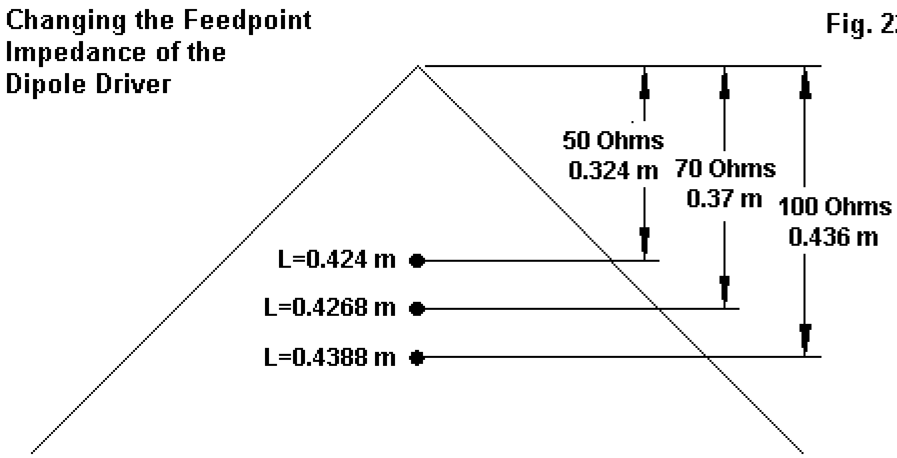

Because the mutual coupling between the reflector and the driver decreases with additional distance between the driver and the reflector surfaces, we find that the dipoles grow longer as they move away from the apex. More significantly, the lessening of mutual coupling also increases the SWR bandwidth, as shown in **Fig. 23**. For each curve, the SWR reference is equal to the resonant impedance of the driver.

Fig. 23

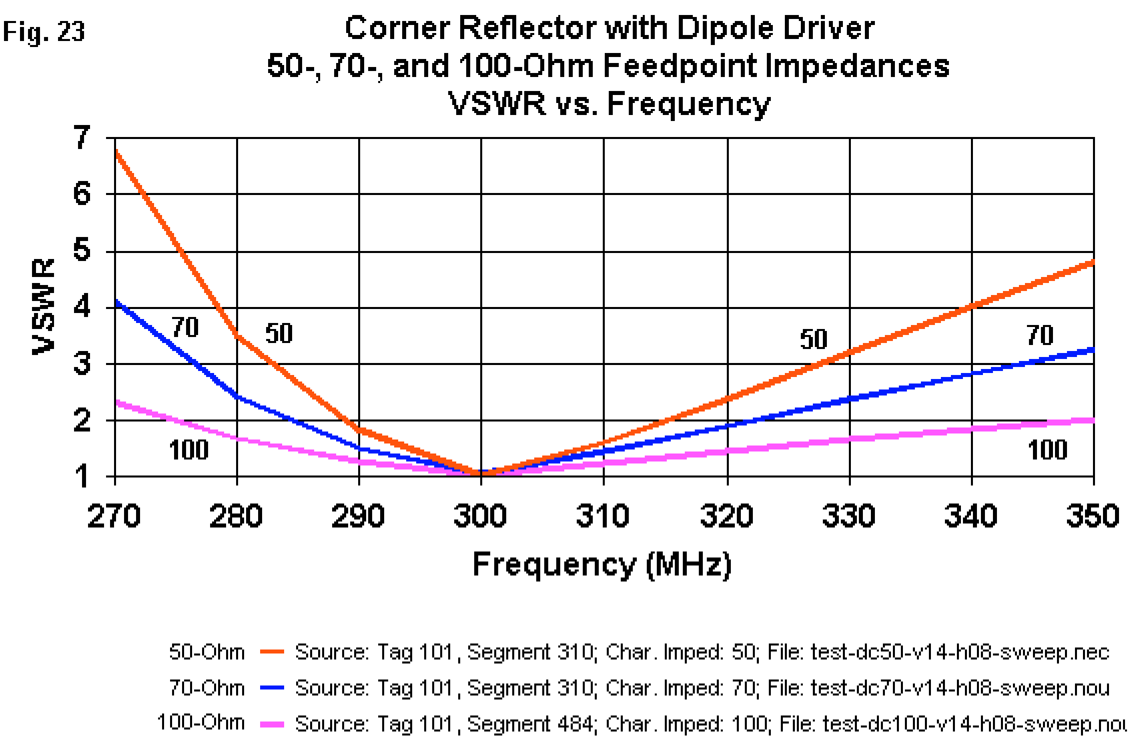

The test used a side length of 0.8 wavelength and a vertical height of 1.4 wavelengths. However, the independence of the driver impedance from the reflector size suggests that we would obtain similar results for other reflector structures. The 8-mm dipole yields a 9% SWR passband when set for a 50-Ohm feedpoint impedance. If we are willing to work with 70-Ohm cables--such as surplus television cables and hard lines--we can increase the SWR passband by 40% to a total value of 12.7%. If a 100-Ohm impedance is not troublesome, the passband expands to 25%, that is, a 2:1 100-Ohm SWR that extends from about 275 to 350 MHz. Such a passband is sufficient to cover the entire FM broadcast band (about 20%, using the usual 88-108-MHz markers). The following tabular lines show to what degree we gain or lose anything from test-frequency performance.

Dipole Diameter And Impedance	Gain dBi	Front-to-Back Ratio dB	E-BW degrees	H-BW degrees	Impedance R +/- jX Ohms
8-mm--50-Ohm	11.42	38.27	46	54	49.63 - j1.56
8-mm--70 Ohm	11.37	37.86	46	54	70.04 - j0.19
8-mm--100 Ohm	11.28	36.08	46	54	100.15 - j0.17

Contrary to some corner reflector literature, gain does not increase with the use of higher impedance drivers and larger distances between the driver and the 90-degree corner apex. However, the decrease in both gain and front-to-back ratio is below the level of operational detectability.

Rod Reflectors

We may replace the wire-grid reflector and by extension the solid surface or closely spaced screen that it simulates with a set of rods in the E-plane of the driver. As established for planar reflectors, a rod diameter of 0.03 wavelength with a spacing between rods of 0.1 wavelength allows a virtual perfect fit of a driver moved from one type of reflector to the other. With the rods in place, I surveyed rod reflectors ranging from 1.0 to 2.0 wavelengths in vertical height, with side lengths ranging from 0.5 wavelength up to 3.0 wavelengths. The vertical increment was 0.2 wavelength, and the side-length increment was 0.1 wavelength.

The following table summarizes the results for each vertical height test in terms of the side length yielding maximum gain. "F-S" means free space, and "wl" means wavelength(s). Side lengths for the wire-grid reflectors may not be exact, since the model sizes forced the use of a larger increment between samplings.

Reflector	Wire-Grid Model		Rod Reflector		Difference
Vertical Length wl	Peak F-S Gain dBi	Side Length wl	Peak F-S Gain dBi	Side Length wl	Relative to Wire-Grid
1.0	12.78	2.8	11.59	2.0	-1.19
1.2	13.16	2.4-2.8	12.94	2.5	-0.22
1.4	13.48	2.4	13.73	2.6	+0.25
1.6	13.73	2.4	13.41	2.0-2.3	-0.32
1.8	13.77	2.4	13.33	2.1-2.3	-0.44
2.0	13.57	2.4	13.39	2.3-2.4	-0.18

For all reflector vertical heights, the rod reflector returns a slightly lower gain--except for a vertical height of 1.4 wavelengths. Wire-grid maximum gain occurs at a height of 1.8 wavelengths. However, a rod reflector shows peak gain at a height of 1.4 wavelengths. Not only is this height a near-resonant 3/2-wavelengths, but as well, it is somewhat unstable, as revealed in the gain curves in **Fig. 24**. Note the ripples in the gain curve for 1.4 wavelengths, and the slighter irregularities at long side lengths for the 1.2-wavelength curve. These curves reveal significant parasitic effects in addition to normal reflector illumination.

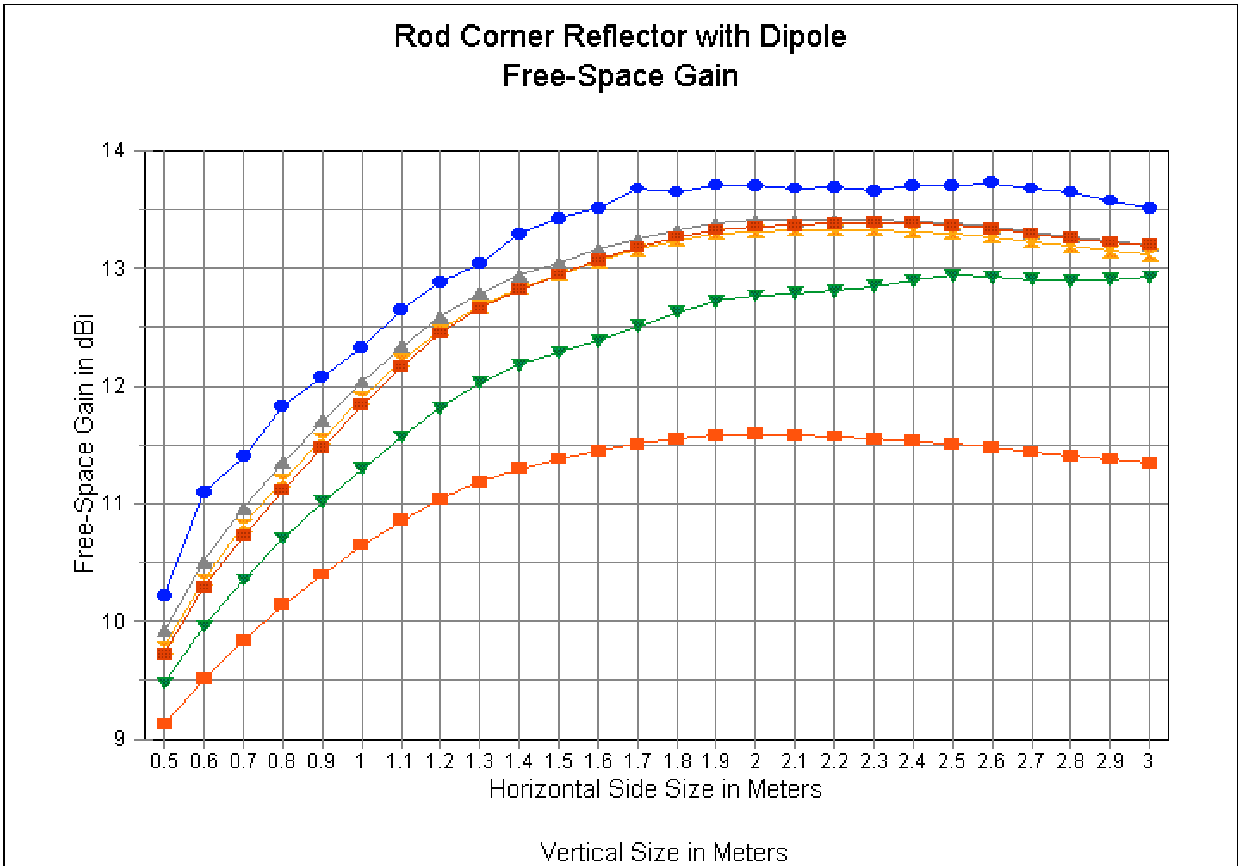

Fig. 24

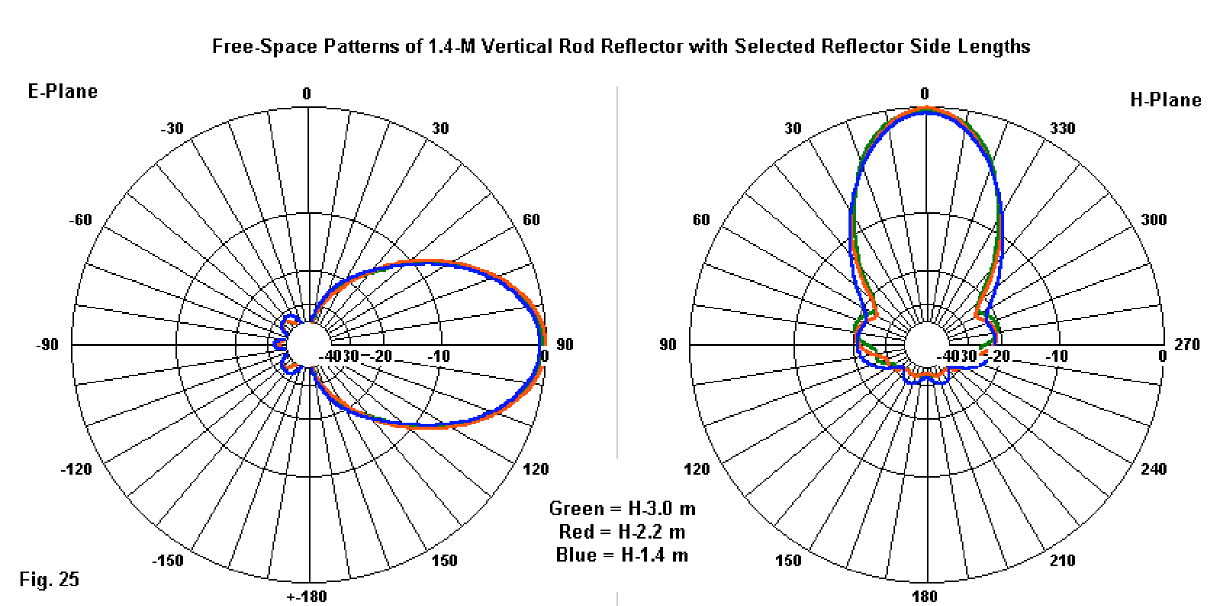

Fig. 25

Relative to wire-grid patterns for maximum gain, the patterns for a maximum gain rod reflector do not exhibit any significant anomalies. **Fig. 25** overlays patterns for a 1.4-wavelength reflector with side lengths of 1.4, 2.2, and 3.0 wavelengths. At most, we obtain slight nulls in the H-plane patterns at longer side lengths, but no increase in the strength of the pattern in directions close to 90 degrees from the forward lobe heading.

The end result of this exploration of basic rod reflector properties differs from what we saw in planar reflectors. Planar reflectors showed a uniform maximum gain height of 1.2 wavelengths, regardless of construction or driver type. In contrast, rod reflectors require a greater vertical dimension for maximum gain. With relatively uniform illumination, wire-grid reflectors need about 1.8 wavelengths. However, with a combination of standard illumination and parasitic effects, rod reflectors show maximum gain at 1.4 wavelengths. However, both types of reflectors require about 2.4 to 2.6 wavelengths of side length.

Reflector Modifications

There are numerous ways in which we can modify the standard 90-degree reflector in an effort to either simplify construction or improve performance. Let's examine a few options that have appeared from time to time in the literature.

1. *Narrowing the Corner Angle*. Since earliest days, we have known that a 90-degree corner angle does not yield the highest gain. Rather, it is simply a convenient angle with which to work and yields good, if not superlative results. **Fig. 26** shows some of the alternative angles that we might use profitably.

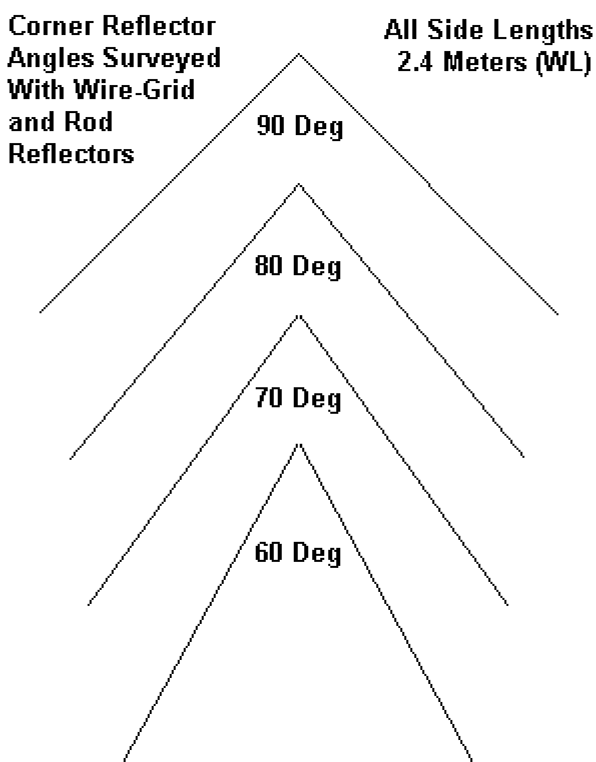

Fig. 26

To see what we might gain, if anything, from a narrower corner angle, I surveyed both wire-grid and rod corner reflectors using 1.4-wavelength vertical reflectors having a side length of 2.4 wavelengths. **Fig. 27** shows the results in terms of the free-space forward gain.

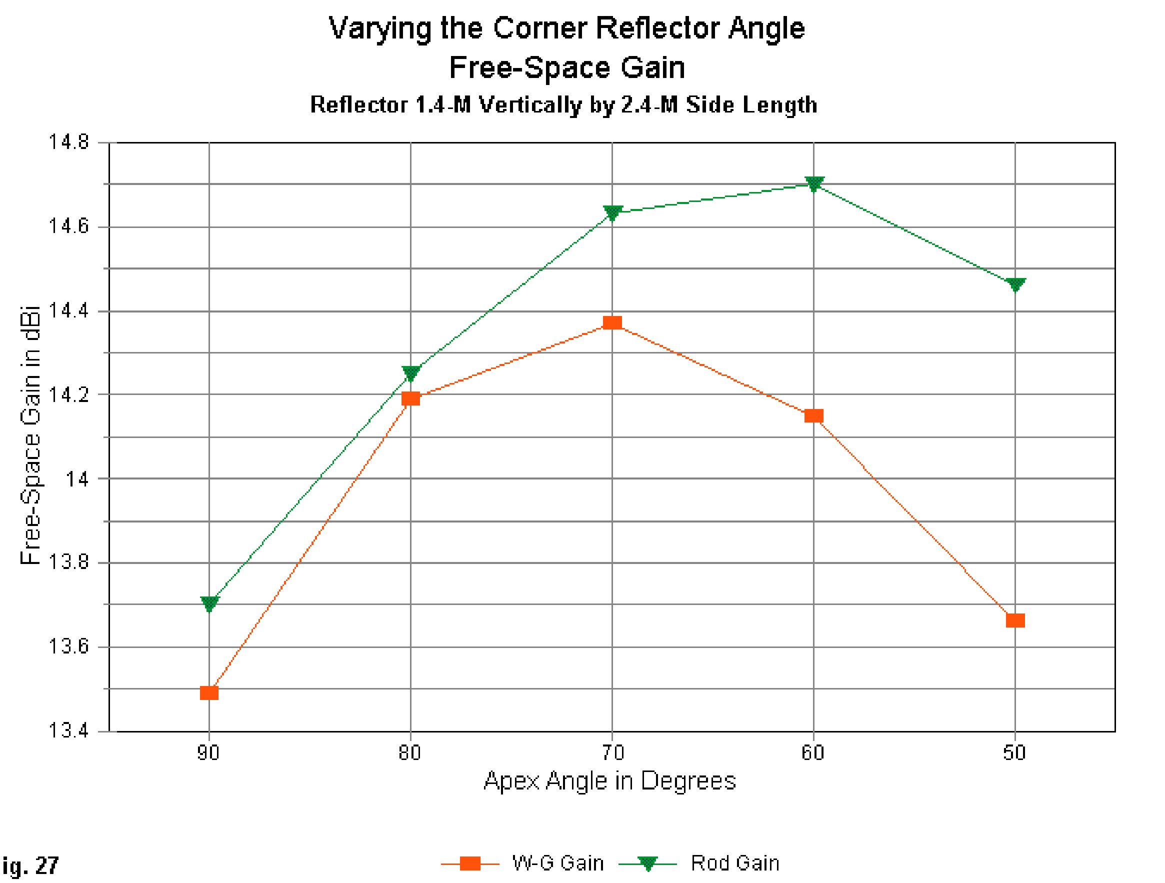

Fig. 27

Wire-grid gain peaks at an angle of about 70 degrees, but the rod-reflector requires a narrower angle for peak gain, something just over 60 degrees, if we read the peak values correctly. The following table provides a more detailed look at comparative numbers as we reduce the angles for both types of reflector.

Space wl	Length wl	Angle deg.	Gain DBi	Front-Back Ratio dB	E-BW deg.	H-BW deg.	Impedance R +/- jX Ohms
Wire-Grid Reflectors							
0.325	0.4248	90	13.49	38.00	40	34	50.10 + j0.20
0.364	0.4226	80	14.19	46.29	38	30	50.11 + j0.20
0.4135	0.4202	70	14.27	45.35	38	28	50.10 + j0.03
0.480	0.4174	60	14.15	43.40	38	32	50.20 + j0.03
0.573	0.4140	50	13.66	32.86	40	36	50.03 + j0.03
Rod Reflectors							
0.323	0.4248	90	13.70	34.05	42	36	50.22 - j0.03
0.361	0.4226	80	14.25	36.69	40	32	50.18 - j0.11
0.410	0.4202	70	14.63	40.55	38	30	50.08 + j0.02
0.4765	0.4172	60	14.70	43.41	38	30	50.09 - j0.21
0.569	0.4140	50	14.46	38.77	38	34	49.88 + j0.03

As one should expect, the smaller the angle of the corner reflector, the greater the spacing of the driver from the apex for a fixed 50-Ohm resonant impedance. However, because the reflector surfaces are "closing in" on the driver, the mutual coupling is greater and the resonant length of the dipole grows shorter. That same coupling yields stronger parasitic effects on the rod reflector than on the wire-grid model. Hence, the rod-reflector using 1.4-wavelength rods produces higher gain at a tighter angle. The stronger mutual coupling also shows up in narrowing SWR curves as the angle grows smaller. **Fig. 28** shows representative curves at 90, 70, and 50 degrees for rod reflectors.

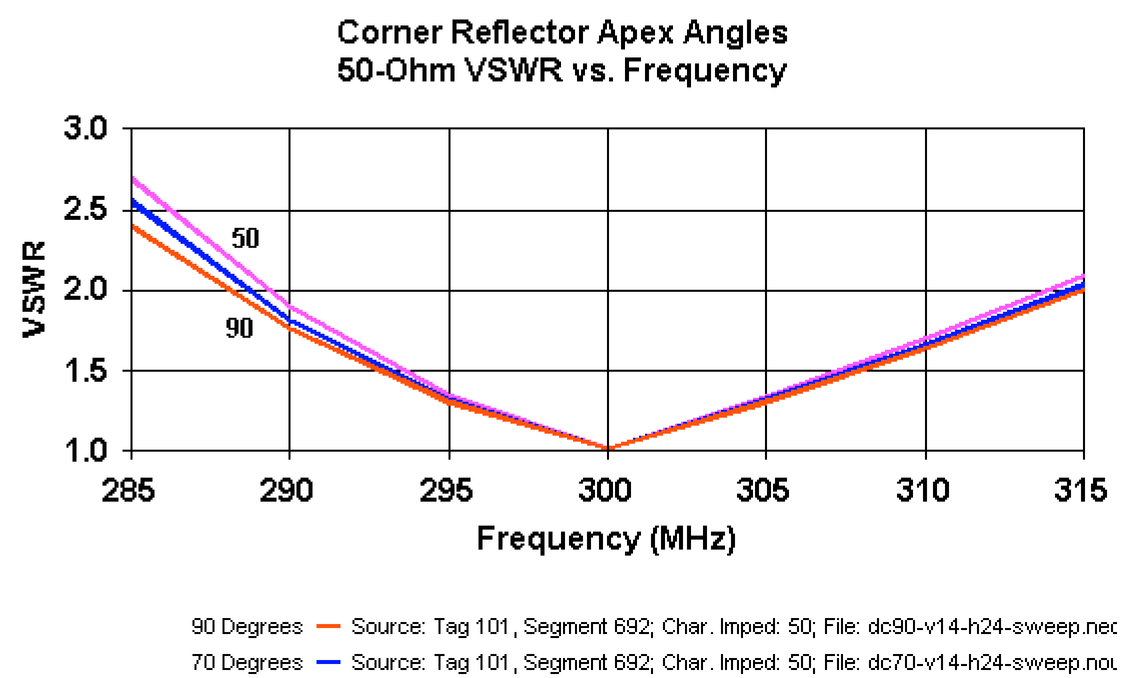

Fig. 28

2. *Fold-In Apertures*. An alternative to a narrow corner angle is to fold the aperture end of the reflector inward, as sketched in **Fig. 29**. Since there are so many possibilities here, we shall have to satisfy ourselves with a single sample.

Adding a fold-in to a 90-Degree Corner Reflector 1.4-M Vertically With a Basic Side Length of 2.3 M: Each fold-in step is 0.1-m forward, but no wider than the initial aperture (3.25 m).

No. of Fold-In rods	Free-Space Gain dBi	Front-to-Back Ratio dB	E-BW degrees	H-BW degrees	Impedance R +/- jX Ohms
No added rods	13.66	35.78	42	36	50.22 - j0.02
1 fold-in rod	13.79	32.97	42	34	50.26 - j0.03
2 fold-in rods	13.88	35.43	42	32	50.30 - j0.13
3 fold-in rods	14.13	38.59	40	30	50.12 - j0.29
4 fold-in rods	14.47	31.40	38	26	50.01 - j0.07

Folding in the aperture has the effect of narrowing the corner angle, while preserving the working space of the 90-degree corner. The driver has not moved with the varying fold-ins.

Standard and Fold-In Reflector Outlines

Fig. 29

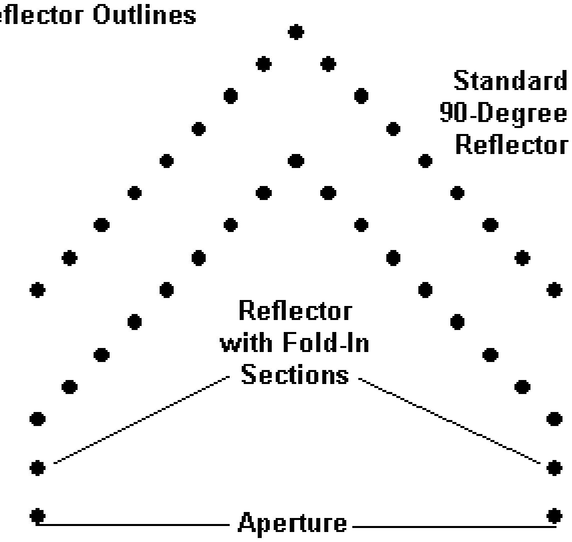

The test series has used rod reflectors 1.4 wavelength high. Since the maximum gain of such a reflector occurs with a 60-degree angle, I added a single rod to the side length in standard fashion and then did a fold-in instead. The following table shows the results.

Options for a 60-Degree Corner Reflector 1.4-M Vertically With a Basic
Side Length of 2.4 M: A. Extending the side length to 2.5 M, or B. Adding a fold-in rod.
Each fold-in step is 0.1-m forward, but no wider than the initial aperture (3.0 m).

No. of Fold-In rods	Free-Space Gain dBi	Front-to-Back Ratio dB	E-BW degrees	H-BW degrees	Impedance R +/- jX Ohms
60 deg, 2.4-m side	14.70	43.40	38	30	50.37 + j0.15
60-deg, 2.5-m side	14.80	42.65	38	30	50.43 + j0.17
60-deg, 2.4+fold-in	14.80	39.41	38	30	50.47 + j0.17

Adding 0.1-m to each side increased the gain by about 0.1 dB. Note that the fold-in did no better, but actually shows a slight reduction in the front-to-back ratio. The beamwidths do not change for either modification relative to their initial values. The data suggest strongly that there is a limit to the amount by which fold-in structures can improve the performance of a corner array. When the effective angle produced by the fold in approaches or reaches the corner angle of optimal performance for a plane-sided corner array, improvements will disappear. Since a 90-degree corner is distant from the smaller angle that marks the maximum gain that might be achieved for a given side-length, fold-ins show excellent potential for improved performance. However, if we begin with the optimal angle for maximum gain, there will be little difference between a fold-in and a simple side extension.

3. *Trough Reflectors*. A recurrent suggestion in corner reflector literature is the trough reflector. We cut off the apex region of the reflector and thereby gain a flat surface for reflector mounting. **Fig. 30** shows the general idea. Unfortunately, corner-reflector literature is vague on what we might expect by way of performance advantages or disadvantages from such a reflector design. As a result, I performed a preliminary survey of troughs that cut off varying portions of the reflector apex. I then reset the driver for a 50-Ohm resonant impedance and registered the performance results.

Fig. 30

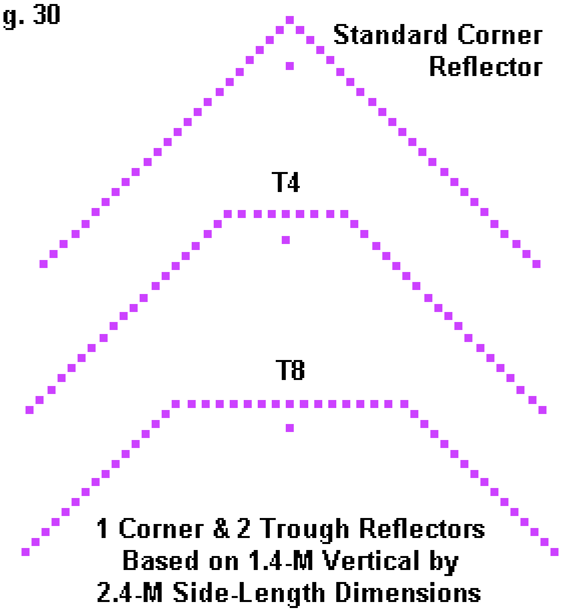

The following table records the results of the survey. The model identification records the amount cut off from the apex, where T2, for example, means that 0.2 wavelength has been removed and replaced by a flat surface. The largest troughs result in a split forward H-plane lobe that has a central null that is greater than 3 dB.

Trough Model	Free-Space Gain dBi	Front-to-Back Ratio dB	E-BW degrees	H-BW degrees	Impedance R +/- jX Ohms
T0	13.70	34.05	42	36	50.22 - j0.03
T2	13.56	30.45	42	34	49.97 - j0.10
T4	13.74	27.75	44	30	49.88 - j0.16
T6	12.80	27.84	42	36	50.01 - j0.22
T8	11.12 split	23.89	56	68	49.97 + j0.04
T10	11.51 split	18.00 (approx.)	88	68	49.95 - j0.23

The telltale symptom of the general failure of trough reflectors to perform up to general corner reflector standards is the spacing of the driver from the surface for a 50-Ohm impedance. T0, the standard corner reflector, spaces the dipole 0.324 wavelength from the corner apex. However, all trough models require a spacing of 0.175 wavelength, the same distance as from a planar reflector. Beyond the T4 level, a trough reflector offers distinct gain deficits. Even at the T2 and T4 levels, the trough reflector front-to-back ratio is lower than for a true corner reflector.

4. *Enhancing Parasitic Effects*. This survey is not the only place in which the parasitic effects of rod reflectors have gained notice. John Regnault (G3SWX) and John Sager (G0ONH) have been working on enhancing those effects, using a reflector with a 1.4-wavelength height and 2.4-wavelength sides. The British reflectors also use a 70-75-degree angle with mild aperture fold-ins. However, the unique feature of their continuing work is the fact that they have altered the length of individual reflector rods as a means of increasing the gain of the array. In some cases, they have shortened individual rods to just over ½ wavelength. In other cases, they have removed inactive rods altogether.

Since each array that they design uses a different combination of rod lengths, a systematic survey is not possible. At most, in these pages, we can sample the patterns of one of their designs. See **Fig. 31**.

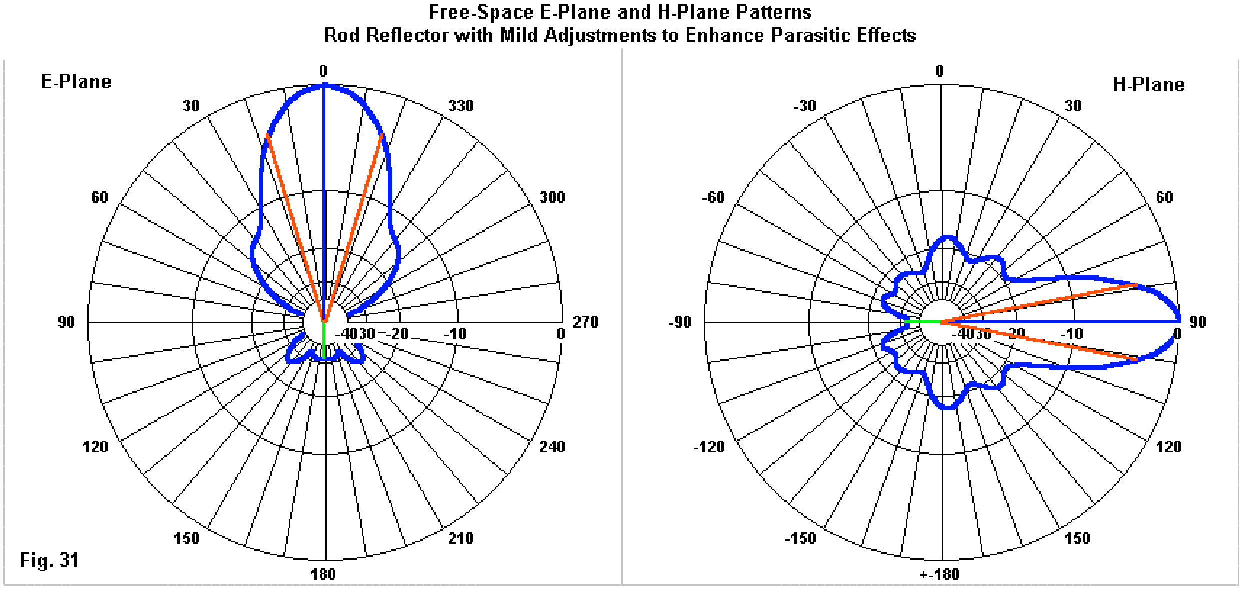

Fig. 31

The patterns clearly show the hybrid nature of the modified reflector structures. The beamwidths are typical of corner arrays, but the emergent sidelobes are more typical of parasitic arrays, such as Yagis. The following table compares the performance reports of a standard 70-degree corner reflector and one of the enhanced parasitic designs.

Array	Angle Degrees	Gain dBi	Front-Back Ratio dB	E-BW degrees	H-BW degrees	Impedance R +/- jX Ohms
Standard	70	14.63	40.55	38	30	50.08 + j0.02
Corn6A	75	15.66	32.13	34	22	49.91 - j0.04

Recent correspondence suggests that newer versions of the enhanced parasitic corner reflector have raised the free-space gain to about 17.4 dBi. These developments will bear watching when they appear in print.

Bandwidth 1--Collinear Drivers

One trait for which numerous corner reflector designers have striven is a wide SWR bandwidth. One route toward that goal is to increase the spacing of the driving dipole from the corner apex, accepting the increased impedance as a consequence. A 100-Ohm placement yields a 2:1 SWR bandwidth of about 25% relative to the design frequency. We obtained a similar result using a planar array with a broadside array of two dipoles by setting each at 100 Ohms and then phase feeding the pair. However, a corner reflector--even one as wide as 90 degrees--does not accept such an array as a driver, since there is no way to optimize the spacing from the apex while maintaining an optimal distance between the dipoles and the reflector surfaces.

There is an alternative solution. We may arrange the driving pair of dipoles as a collinear array. This configuration preserves the driver-to-reflector spacing and allows a pair of 100-

Ohm phase lines to equally feed the two dipoles. **Fig. 32** shows the general layout for such a corner reflector array.

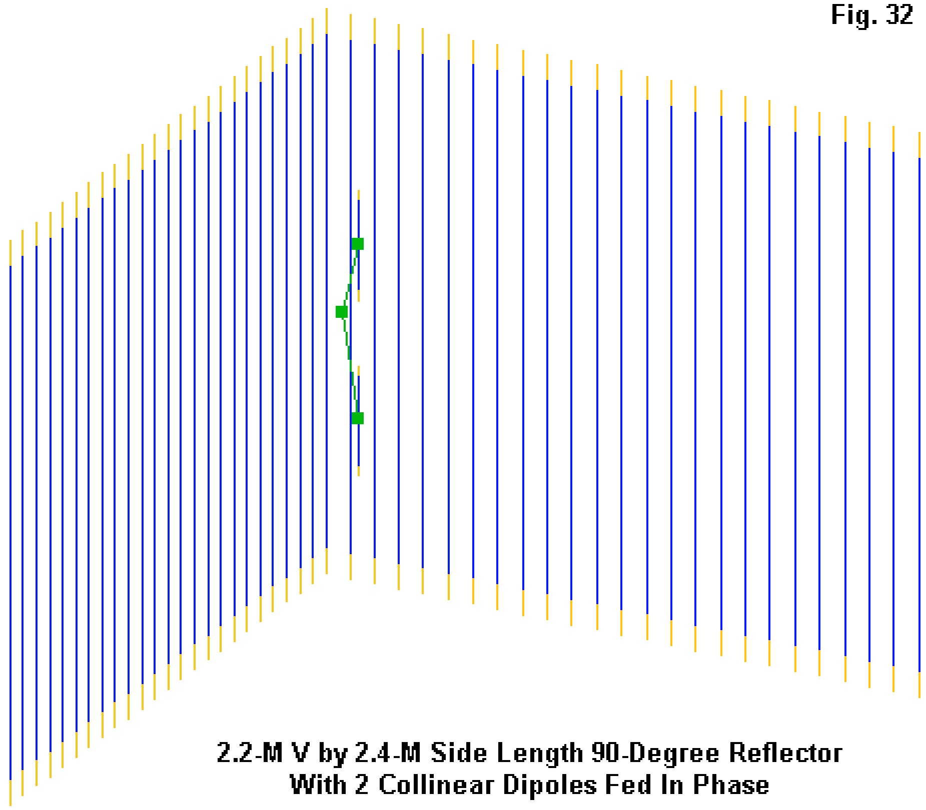

In the test models, the inner dipole ends are 1/4-wavelength apart. The spacing from the apex is 0.393 wavelength to give each dipole a resonant 100-Ohm impedance. In concert with the broadside planar array, the individual feedpoints connect to a central feedpoint via 100-Ohm transmission lines. The parallel combination at the junction provides a good match for 50-Ohm cable. Each dipole is 0.433-wavelength long, and so the overall length of the driver assembly is 1.116 wavelengths. The dipoles use the 8-mm diameter also used for single dipole drivers. Since the test aims only to test the principle, I made no effort to space the dipoles from each other for maximum possible gain.

A preliminary survey using reflector vertical dimensions of various sizes yielded the fact that maximum array gain occurred with a height of 2.2 wavelengths. The extension of the reflector beyond the collinear dipole limit is about 0.54 wavelength on each side, close to the extension value required for a single dipole and a rod reflector. For the configuration used in the test, maximum free-space gain was 14.95 dBi on the design frequency, about 1.2 dB higher than for a single dipole driver using a rod reflector 1.4 wavelength vertically and also 2.4 wavelengths on each side.

Fig. 33 shows the free-space gain and front-to-back performance of the array across the frequency sweep from 270 to 350 MHz. The gain peaks at 15.2 dBi just above the design frequency at 310 MHz, while the front-to-back ratio shows its lowest values on either side of the peak gain frequency. However, the 180-degree front-to-back ratio never drops below 37 dB.

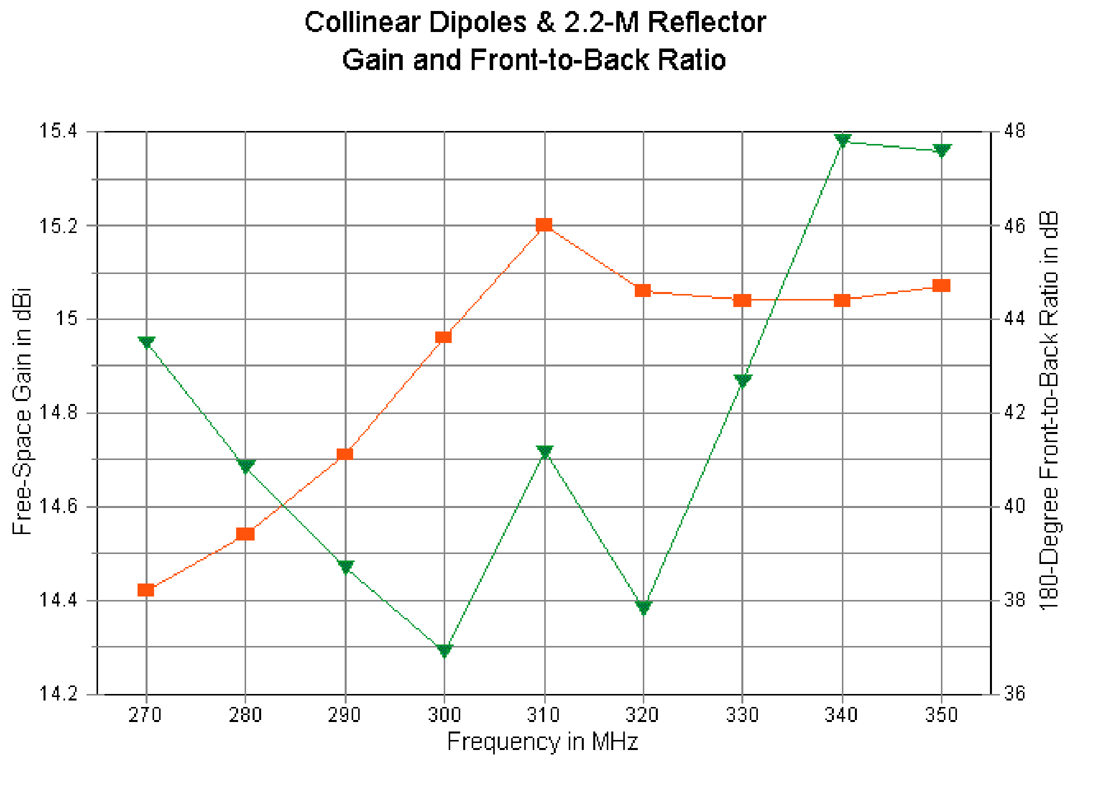
Collinear Dipoles & 2.2-M Reflector
Gain and Front-to-Back Ratio
Free-Space Gain in dBi
180-Degree Front-to-Back Ratio in dB
15.4
15.2
15
14.8
14.6
14.4
14.2
48
46
44
42
40
38
36
270
280
290
300
310
320
330
340
350
Frequency in MHz
Gain dBi
F-B dB

Fig. 33

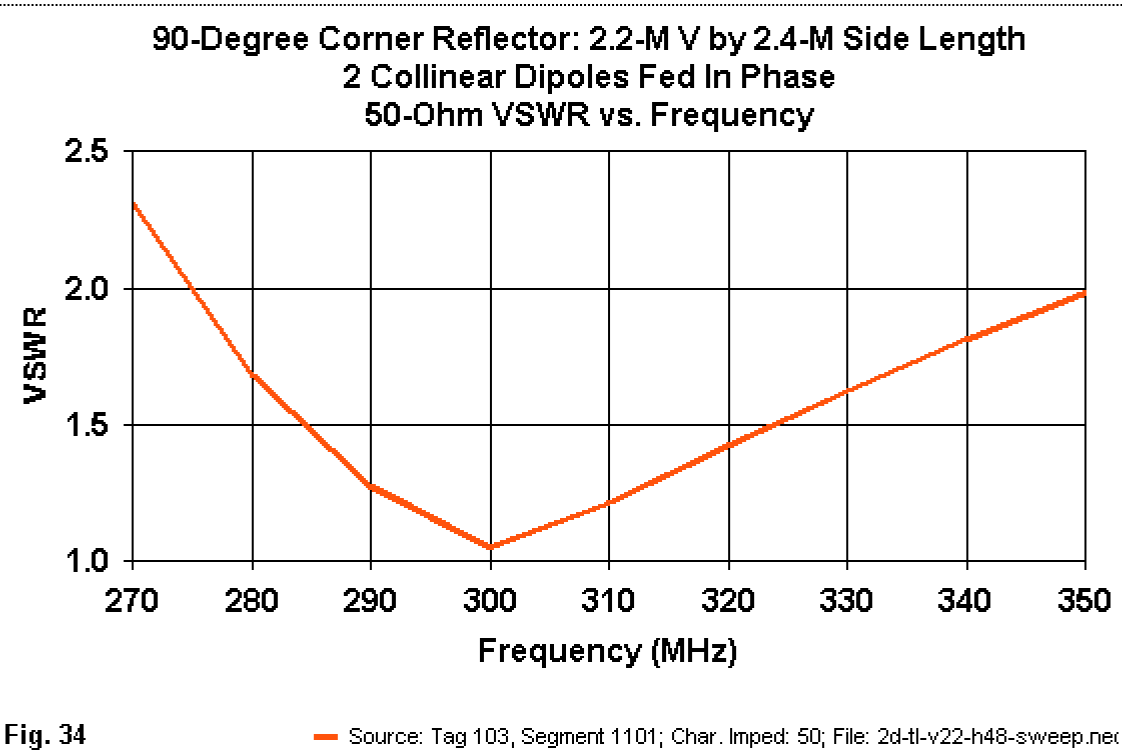
90-Degree Corner Reflector: 2.2-M V by 2.4-M Side Length
2 Collinear Dipoles Fed In Phase
50-Ohm VSWR vs. Frequency
VSWR
2.5
2.0
1.5
1.0
270
280
290
300
310
320
330
340
350
Frequency (MHz)
Source: Tag 103, Segment 1101; Char. Imped: 50; File: 2d-tl-v22-h48-sweep.nec

Fig. 34

The 50-Ohm SWR curve appears in **Fig. 34**. The acceptable (2:1) SWR level exists from 275 to 350 MHz, a 75-MHz passband. Expressed in other terms, we have a 25% passband with respect to the 2:1 50-Ohm SWR standard when referenced to the design frequency. Not only is the feedpoint impedance well behaved across this range, but as well, the E-plane and H-plane patterns are paradigm examples of what a corner reflector can achieve. **Fig. 35** provides a pair of samples from the design frequency.

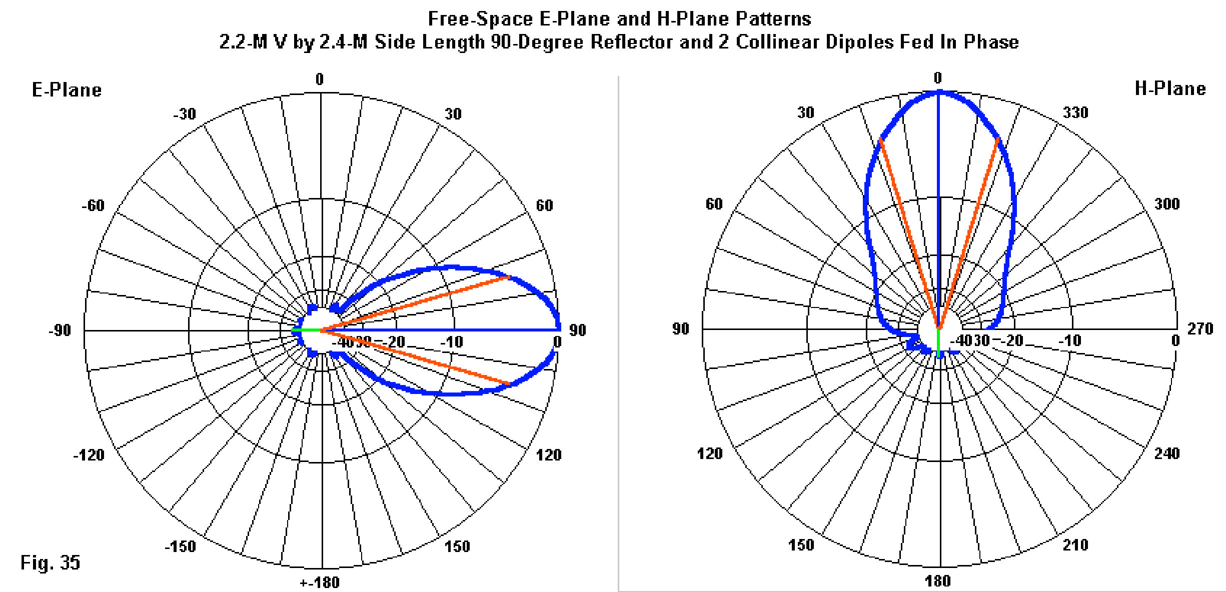

Fig. 35

Bandwidth 2--Brown-Woodward Bent Fan Dipole Drivers

An alternative means of increasing the SWR bandwidth over a simple dipole is to use a fan dipole. When each side of the dipole fans out at about a 45-degree angle, with an end cross piece, the fan reaches its maximum bandwidth. However, within the corner reflector, we can only achieve a bandwidth of about 25% or so, about the same as with a pair of collinear drivers. However, we can reach this plateau in SWR bandwidth using reflectors that are more standard in vertical size.

In the 1950s, a commercial television corner reflector emerged claiming 2:1 frequency coverage to supply the need for the new UHF channels in pre-cable-television days. The array was modest in size, using a vertical dimension of about 1.2 wavelengths at the mid-range frequency and with sides also about 1.2 wavelengths. However, the key to the array was the Brown-Woodward bent "bow-tie" dipole driver. The dipole not only fanned out, but also bent part of each fan end forward by 45 degrees. The result was a fanned section on each side of the feedpoint that was parallel to the surfaces of the 90-degree corner reflector.

To test both the flat and bent fan dipoles, I created models of them, using 8-mm diameter wire to simulate as best possible something close to the solid surface of the Brown-Woodward driver. **Fig. 36** shows the outlines of the models. The bent fan required a central wire from end to end to create simulated plane surfaces at 90 degrees to each other. The result was a somewhat elevated average gain test. However, in performance reports, I have corrected the NEC reports accordingly. Both drivers are 0.49-0.50 wavelength from the corner apex. The flat version is 0.24-wavelength long and 0.11wavelength each side of the centerline. The bent version is 0.262-wavelength long and 0.075 wavelength each side of the centerline.

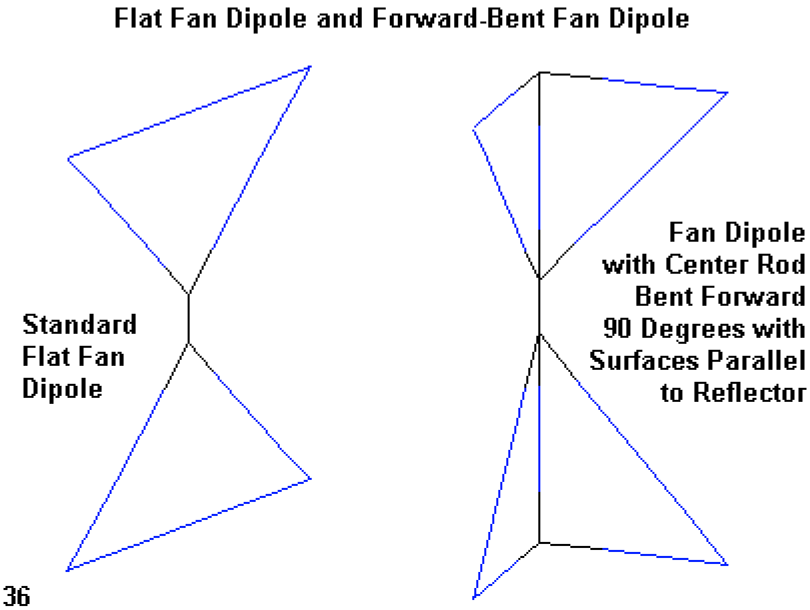

Fig. 36

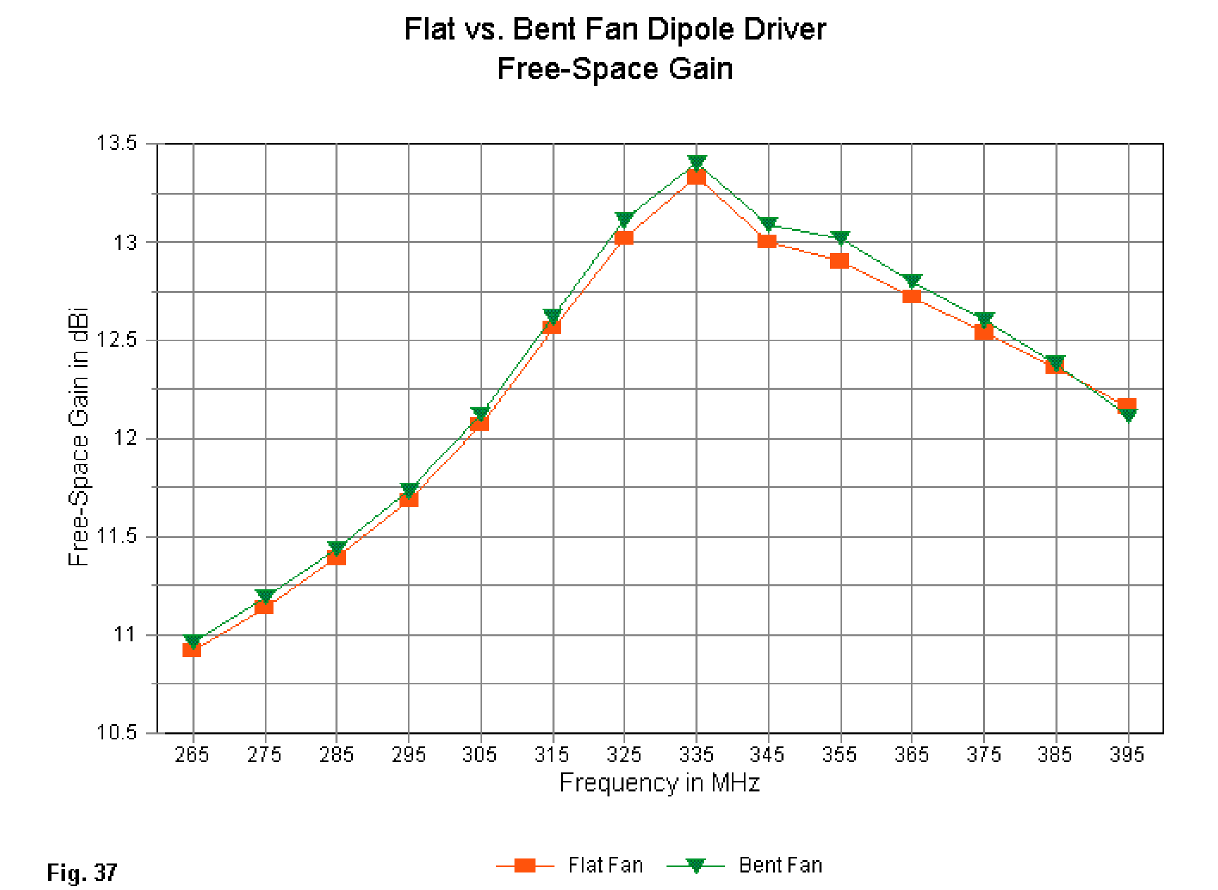

Fig. 37

Fig. 37 shows the gain for both the flat and bent dipole drivers across a frequency sweep from 265 to 395 MHz. Note that there is no significant performance difference between the two drivers with respect to gain, despite the difference in element arrangement. The front-to-back curves are equally congruent, but the differential varies from 2 to 4 dB in favor of the flat fan dipole driver.

The difference between the two fan drivers shows up most clearly in the 50-Ohm SWR curves, as revealed in **Fig. 38**. For the bent dipole driver, the 2:1 SWR passband edges are 265 MHz at one end of the range and 385 MHz at the other end. This 120-MHz range is a 40% bandwidth relative to the design frequency or about 37% relative to the center-frequency of the defined passband. The bent dipole clearly provides a very significant increase in the passband relative to what a flat fan dipole can provide. According to the literature, the difference is a function of the fact that the planes of the bent fan parallel the planes of the reflector.

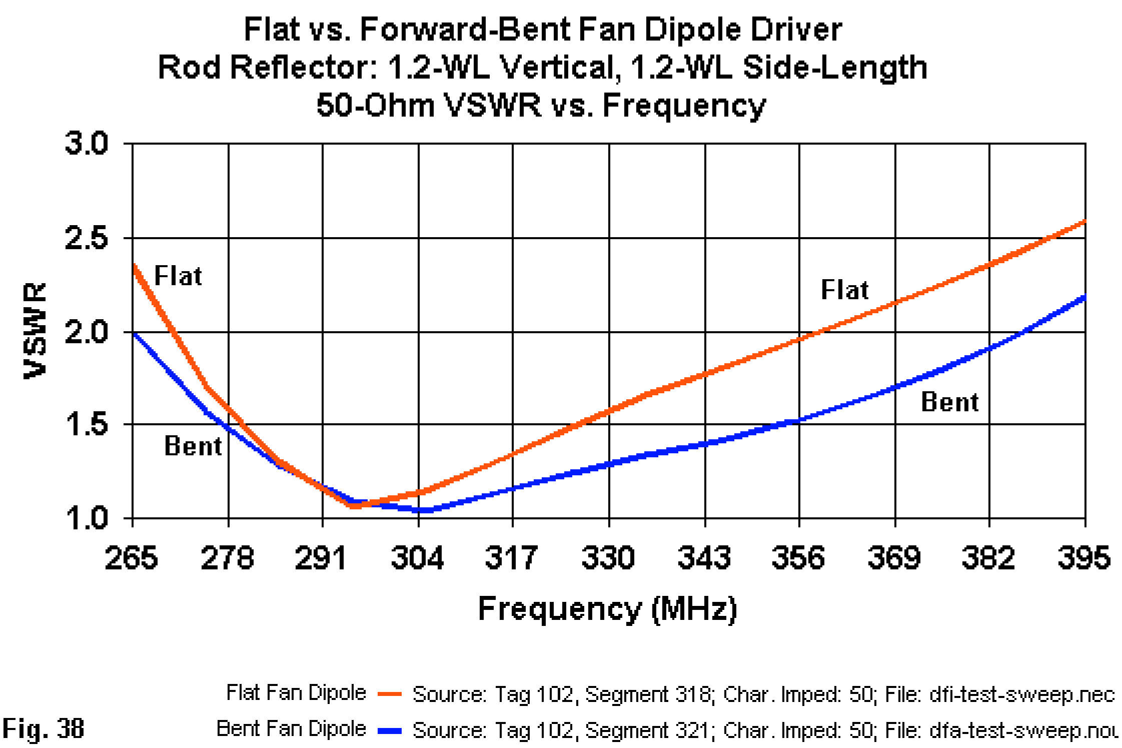

Fig. 38

The passband increases further if we re-design the bent fan dipole for a higher impedance. Preliminary models have come close to the original 300-400-Ohm impedance and have also shown considerable improvement over the already wide 50-Ohm passband. However, present models are not yet reliable enough to be more than suggestive in this regard.

To answer the question of what gives the bent fan dipole its wide passband within the framework of a corner reflector, we must examine the impedance values more closely. Both fan dipoles show a normal reactance progression, although the limits for the bent version are somewhat narrower than for the flat fan driver. However, that difference alone is insufficient to account for the large increase in SWR bandwidth. To understand the bandwidth increase, we must examine the behavior of the feedpoint resistance across the swept frequency. **Fig. 39** supplies a comparative graph of the feedpoint resistance values for both types of fan drivers within the corner reflector.

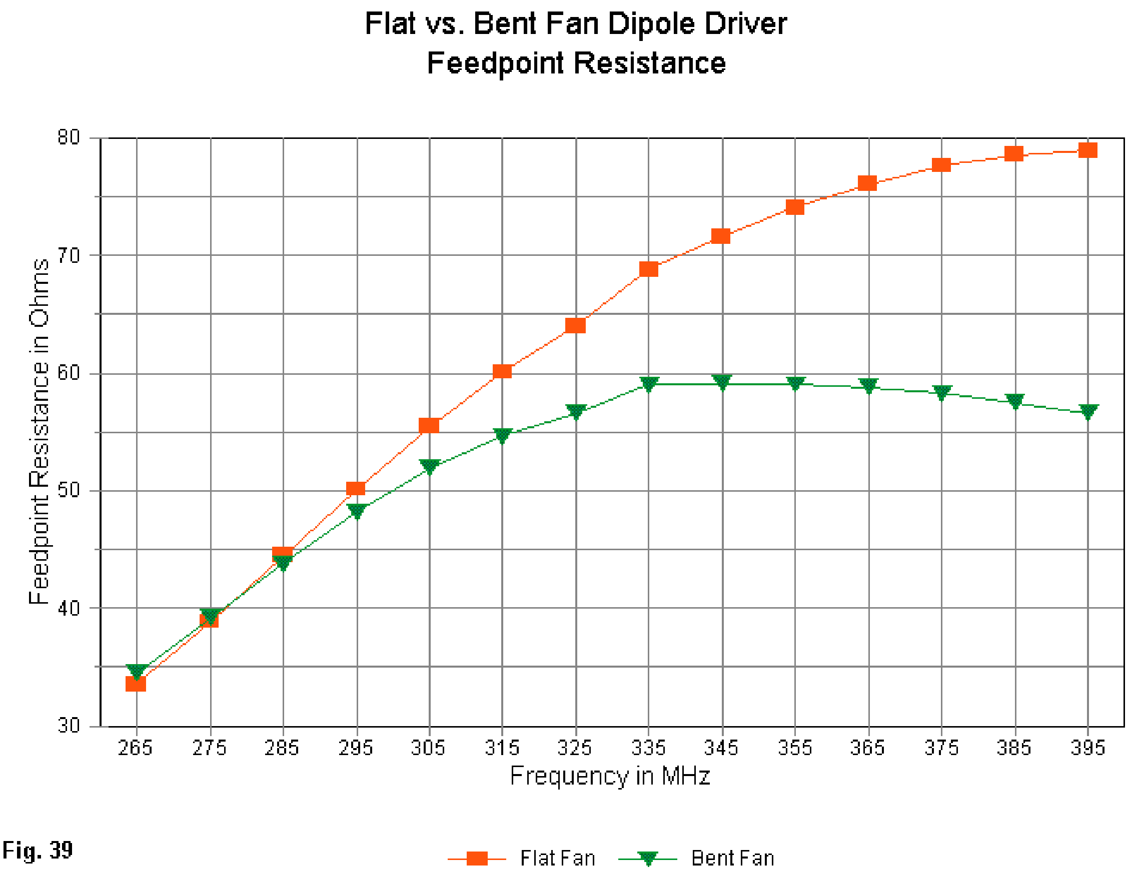

Fig. 39

The curve for the flat fan shows a very normal curve that climbs steadily upward, although it slows the rate of climb as the frequency approaches the upper limit. The bent-fan curve tells a much different tale, as it reaches a maximum value at about the same frequency as the point of highest gain. Then, as we further increase the frequency, the curve levels off and actually declines. The parallel planes of the driver and the reflector increase coupling between the two surfaces as we increase frequency, with the normal result of a lower overall impedance in the driven element. The effect is sufficient to partially counteract the tendency toward higher impedance values with increasing frequency, at least enough to broaden the SWR bandwidth.

Our little experiment--even with all of its differences from the original antenna--suffices to uncover the principle of the Brown-Woodward bow tie's prowess in serving as the focal point for a very-wide-band corner reflector. Indeed, controlling the width of the fan's projections, with consequential adjustments to its overall length, would give the designer a degree of further control over the bandwidth. In addition, one might also experiment with the angle of bend or, in other words, the level of parallelism between the driver and reflector planes as another means of controlling the bandwidth.

The data that we have so far shown involve rod reflectors. The bent-fan dipole driver is equally applicable to a wire-grid reflector that simulates a solid surface or a closely spaced screen. However, we should not expect identical performance curves. **Fig. 40** compares the free-space forward gain of the same bent-fan driver in the 1.2-wavelength vertical rod reflector that we have been using and in a wire-grid reflector that is 1.4 wavelengths vertically. Both have 2.4-wavelength sides.

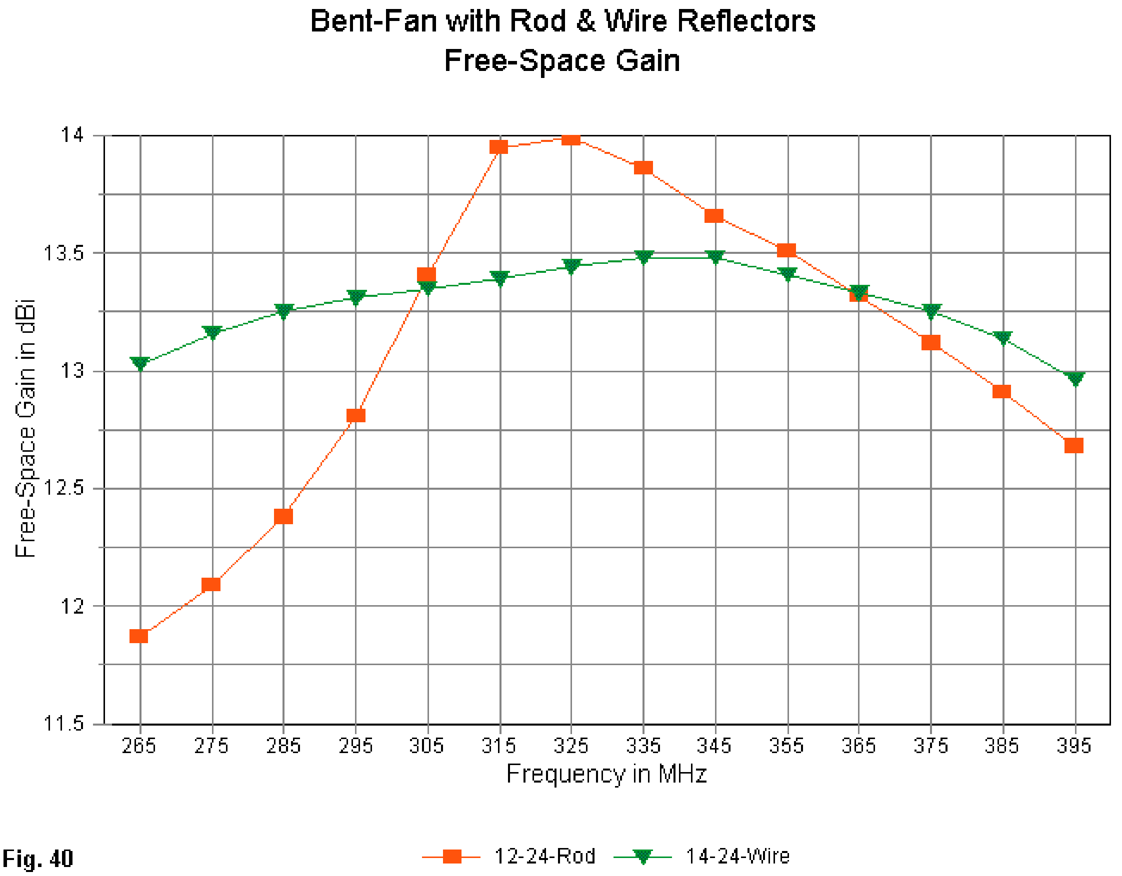

Fig. 40

Both reflectors use longer sides than the initial 1.2-wavelength versions used in initial testing. In the rod reflector we obtain a peak gain about 0.5 dB higher than for the shorter side version. However, the gain curve shares its large differential in the minimum to maximum gain value, well over 2 dB. In contrast, the wire-grid model shows a lower peak gain--by about 0.5 dB--but also a much smaller differential between extremes--just over 0.5 dB. Hence, over the entire passband, the wire-grid model shows a higher gain for over 50% of the passband. In the ultimate quest for a wide-band array, both types of reflectors may have suitable applications.

Summarizing Corner Reflectors

Summarizing the properties of corner reflectors is more difficult than doing the same job for planar reflectors. However, certain generalizations do emerge from our survey of these arrays.

1. Because the optimal vertical (E-plane) dimension for 90-degree corner arrays is larger than 1.2 wavelength, the actual size for peak gain depends on the reflector construction. Wire-grid (solid or screen) reflectors show maximum gain with a vertical dimension of about 1.8 wavelengths and a side length of about 2.4 wavelengths. Rod reflectors reach peak gain with a vertical dimension of 1.4 wavelengths and a side length similar to that of wire-grid reflectors.

In both cases, the peak gains are about 1 dB higher than for reflectors with ½ the optimal side length. The limit of this study with respect to side length was about 3.2 wavelengths.

2. E- and H-plane beamwidths tend to be functions of reflector side length when using an optimal vertical dimension. The H-plane beamwidth tends to decrease almost linearly with increases in reflector side length, regardless of the vertical dimension.

3. For a given side length and an optimal vertical dimension, corner reflectors tend to show increases in gain with reductions in the corner angle, with wire-grid version peaking close to 70 degrees and rod versions peaking close to 60 degrees. Wider angles may be enhanced by the use of fold-ins at the array aperture to create a narrower virtual angle while preserving driver-mounting space near the apex.

4. Driver types are limited by the apex corner angle to dipoles, fan dipoles, and collinear arrays of dipoles. The ideal vertical dimension for collinear arrays is one that shows an extension beyond the driver system limits of about 0.5 to 0.6 wavelength on each end of the driver.

5. Corner reflectors show consistent gain and front-to-back curves over a wide frequency range in relative independence of the driver type. The chief limiting factor in frequency coverage for a corner array tends to be the driver SWR bandwidth. Of the various candidates for a wide-band driver, the Brown-Woodward bent fan dipole shows the greatest bandwidth. In most cases, wide-band use requires a reflector size smaller than the size optimal for maximum gain in order to smooth the response over the larger passband. However, large wire-grid reflectors are capable of even response over a wide frequency range.

6. Wire-grid corner reflectors in wide-band use tend to show lower peak gain values but smoother overall passband performance than rod-reflectors. In contrast, rod reflector peak gains rely upon parasitic effects, which have a narrower bandwidth or effectiveness.

7. Rod reflectors with a vertical height of about 1.4 wavelengths may improve array performance by careful adjustment of reflector rod lengths to enhance parasitic effects. These effects may yield up to about 2 dB additional gain from a given reflector size.

8. Corner reflector patterns show clean single-forward-lobe patterns in both the E- and H-planes. Rearward gain is rarely sufficient to warrant concern for rearward lobe structure. With rod reflectors, especially, increased parasitic effects tend to reveal themselves through the development of sidelobes, most prominently in the H-plane, but in extreme cases of reflector modification, also in the E-plane.

9. Once established, the feedpoint impedance of a driver does not vary significantly with changes in the reflector dimensions.

Most of the properties enumerated in this summary list are "new" in the sense of not having a place yet in fundamental literature about corner reflectors. A similar statement is also true of most of the summary of planar reflector properties. Nevertheless, neither list is in any way complete. We have yet much to learn about planar and corner reflector arrays. Perhaps all that this systematic survey of reflector array properties has accomplished is to establish that this class of antenna is well-worth study.

Space precludes a detailed account of the modeling techniques used in the study, not to mention the validation of certain aspects of the modeling effort. However, those details are covered in a running account in the course of the 9-part *antenneX* series from which I extracted the data for this summary report.